arXiv:1601.07528v2 [quant-ph] 24 Aug 2016

Coupled Harmonic Systems as Quantum Buses in Thermal Environments

F. Nicacio[1,*] and F. L. Semião[1]

[1] *Centro de Ciências Naturais e Humanas, Universidade Federal do ABC, 09210-170, Santo André, São Paulo, Brazil*

(Dated: March 1, 2022)

In this work, we perform a careful study of a special arrangement of coupled systems that consists of two external harmonic oscillators weakly coupled to an arbitrary network (data bus) of strongly interacting oscillators. Our aim is to establish simple effective Hamiltonians and Liouvillians allowing an accurate description of the dynamics of the external oscillators regardless of the topology of the network. By simple we mean an effective description using just a few degrees of freedom. With the methodology developed here, we are able to treat general topologies and, under certain structural conditions, to also include the interaction with external environments. In order to illustrate the predictability of the simplified dynamics, we present a comparative study with the predictions of the numerically obtained exact description in the context of propagation of energy through the network.

I. INTRODUCTION

The manipulation of small scale systems is a key feature of quantum technologies and their quantum behavior is an incontestable mark of the success of quantum mechanics. Such control is an important tool to reveal the potential of quantum concepts from a practical point of view as well. In this context, one may mention interacting nanoelectromechanical systems [1, 2] whose harmonic movement of the elements can be used to harness the power of continuous variables (position, momentum, etc) for quantum information purposes. Another important example of a scalable system for exploration of quantum dynamics is the one consisting of trapped ions whose positions are coupled through dipole-dipole interactions [3]. In both cases, one can end up with a practical implementation of a network of interacting harmonic oscillators that are encompassed in the object of study of this paper. Advances in experimental implementations of oscillator networks in the context of optomechanics [4–6] may also be mentioned as potential candidates for implementation of the general results discussed here.

Due to their prominent role in physics in general, and in quantum technologies in particular, networks of coupled harmonic oscillators are a timely topic of interest. In the context of entanglement, for instance, the characterization of equilibrium states were studied in [7]. On the other hand, entanglement dynamics was the subject treated in [8]. Concerning favorable conditions for entanglement propagation, in [9], a clever scheme of minimal adjustments of frequencies and coupling constants is developed, which enables highly efficient transfer of entanglement through a linear chain (first neighbor interactions) of coupled harmonic oscillators. Starting from a pure numerical study, they also found a simplified Hamiltonian model (no thermal baths) which allowed analytical progress in the understanding of the high efficiency. This was achieved by using the rationale of the rotating wave approximation (RWA), *i.e.*, the elimination of fast oscillating terms in the interaction picture Hamiltonian when they do not contribute appreciably for the dynamics. Our goal is to expand such an idea of frequency and coupling constants adjustments in many different directions, not explored in [9].

We present here conditions for obtaining simplified reduced models for general configurations or topologies of quadratically coupled systems and, more importantly, we work within the formalism of open quantum systems, allowing us to include the presence of surrounding environments. The contribution here allows one to envision applications of our general results to the study of thermal properties [10–13], nonclassical properties [14] or non-equilibrium thermodynamics [15] in harmonic systems; all of them examples of timely topics of research.

In this work, we show that the indirect or dynamical coupling between two distinct oscillators mediated by a general network, the latter with an arbitrary number of degrees of freedom and topology, can be effectively described by a simplified model containing only a few degrees of freedom, provided the RWA rationale used in [9] is generalized. The first step of the method comprises the diagonalization of the Hamiltonian of the network, which reveals its normal modes. It is here that the symplectic formalism is needed [16–20]. Using this tool, we can provide a case-independent diagonalization, *i.e.*, a general procedure without specification *a priori* of the topology of the network. The following critical point is to careful understand how the external distinct oscillators couple to the normal modes of the network, and this is highly dependent on resonances between normal mode frequencies of the network and the natural frequencies of the external oscillators. When dealing here with topologies which are more complex than a linear chain treated in [9], we must take into account possible degeneracies in the frequencies of the normal modes in order to find the correct effective simplified model. Adding to that, another distinctive feature of our work is the inclusion of an environment in the dynamics. In this respect, we extend the unitary description in [9] to a non-unitary open system treatment of the dynamics following a Lindblad master equation (LME). Obtaining an effective description in terms of just a few degrees of freedom when thermal baths are present is not a trivial task. However, under certain structural conditions, we were able to successfully perform such a simplification as discussed in this work. The designed methodology is suitable for the study of communication and transport across the network and, as an illustration or application, we explore here the phe-

* fernando.nicacio@ufabc.edu.br

nomenon of energy transfer between the external oscillators mediated by the network.

The paper is organized as follows. In section II, we describe the system of interest, namely two external oscillators coupled to a general network of oscillators. We add also the presence of thermal baths. Notation in the scope of the formalism of continuous variables and the dynamical equations for the open system dynamics are also presented in this section. The development of the method to obtain simplified models for the dynamics of the external oscillators is presented in Sec. III. There, we present the mathematical tools of the symplectic formalism needed to perform the diagonalization of the network Hamiltonian and to obtain its normal modes. We also present conditions under which an RWA for the open system can be performed, which enable us to drastically simplify the system dynamics description to a picture with just a few degrees of freedom only. Sec. IV is devoted to an example of the previous simplified description, a linear chain. In the context of quantum technologies and the usefulness of the simplified descriptions, we will study the propagation of energy from a quantum system to another through a quantum bus in Sec. V, where we start with the case of a network (linear chain) with non-degenerate normal modes and then proceed to an interesting example with degeneracy. We end this section with a consideration of a network not obeying the Hooke's law. We then conclude with final remarks and some perspectives of future work in Sec. VI. Additionally, two appendices are dedicated to details about the RWA, which is a fundamental tool used in the work, and to long length analytic expressions.

II. THE SYSTEM AND ITS DYNAMICS

The system we have in mind is depicted in Fig.1. Its temporal evolution will be governed by a LME for the density operator $\hat{\rho}$:

$$\frac{d\hat{\rho}}{dt} = \frac{i}{\hbar}[\hat{\rho}, \hat{H}] + \mathcal{L}(\hat{\rho}), \tag{1}$$

where $\hat{H}$ is the Hamiltonian of the system and $\mathcal{L}(\hat{\rho})$ is the non-unitary part of the dynamics accounting for the environment-system interaction. In the Lindblad scenario, the effect of the coupling between the system and the reservoir appears in Eq. (1) by means of

$$\mathcal{L}(\hat{\rho}) = -\frac{1}{2\hbar}\sum_k \left(\{\hat{L}_{(k)}^\dagger \hat{L}_{(k)}, \hat{\rho}\} - 2\hat{L}_{(k)}\hat{\rho}\hat{L}_{(k)}^\dagger \right), \tag{2}$$

where the different $\hat{L}_{(k)}$ are known as the Lindblad operators, and $\{\hat{A}, \hat{B}\}$ denotes the anticommutator between general operators $\hat{A}$ and $\hat{B}$. The index k of the sum is arbitrary until this point, it records the number of Lindblad operators needed to represent the reservoir interaction with the system.

Let us define the collective operator $\hat{X} := (\hat{\mathsf{x}}^\dagger, \hat{x}^\dagger)^\dagger$ as a column vector corresponding to the positions and the canonical conjugate momenta of the oscillators of the system. In this notation, and with respect to the system depicted in Fig. 1, the

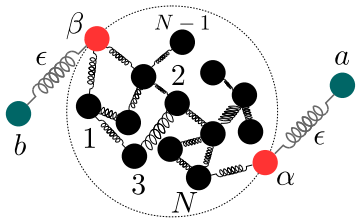


Figure 1. Schematic representation of the system of interest. It consists of a general network of N oscillators where members α^{th} and β^{th} are coupled to two distinctive external oscillators denoted, respectively, as a and b. The coupling constant is ϵ. At this level, we let the coupling constants inside the network completely arbitrary.

operator $\hat{x} := (\hat{q}_1, ..., \hat{q}_N, \hat{p}_1, ..., \hat{p}_N)^\dagger$ accounts for the elements of the newtwork, while $\hat{\mathsf{x}} := (\hat{\mathsf{q}}_a, \hat{\mathsf{q}}_b, \hat{\mathsf{p}}_a, \hat{\mathsf{p}}_b)^\dagger$ represents the external oscillators. The canonical commutation relations among coordinates and momenta are expressed compactly as

$$[\hat{x}_j, \hat{x}_k] = i\hbar\, \mathsf{J}_{jk}^{[N]}, \quad [\hat{\mathsf{x}}_j, \hat{\mathsf{x}}_k] = i\hbar\, \mathsf{J}_{jk}^{[2]}, \tag{3}$$

where

$$\mathsf{J}^{[n]} := \begin{pmatrix} \mathbf{0}_n & \mathsf{I}_n \\ -\mathsf{I}_n & \mathbf{0}_n \end{pmatrix} \tag{4}$$

is the fundamental $2n \times 2n$ symplectic matrix and the blocks I_n and $\mathbf{0}_n$ are, respectively, the n dimensional identity and zero matrices. Even more compactly, one can write

$$[\hat{X}_j, \hat{X}_k] = i\hbar\, \mathsf{J}_{jk} \;\text{ with }\; \mathsf{J} = \mathsf{J}^{[2]} \oplus \mathsf{J}^{[N]}. \tag{5}$$

The label $[n]$ of the above matrices is the number of degrees of freedom and will be omitted if clear in the context.

The Hamiltonian $\hat{H}$ of the global system in (1) contains two parts $\hat{H} = \hat{H}_0 + \hat{H}_I$, where

$$\hat{H}_0 = \tfrac{1}{2}\hat{X}^\dagger \mathbf{H}_0 \hat{X} = \tfrac{1}{2}\hat{\mathsf{x}}^\dagger \mathbf{H}_{\text{e}} \hat{\mathsf{x}} + \tfrac{1}{2}\hat{x}^\dagger \mathbf{H}_{\text{N}} \hat{x} \tag{6}$$

is the sum of the free Hamiltonians of network and external oscillators, and $\hat{H}_I$ describes the interaction of these subsystems. Assuming the standard Hooke's law prescription (springs), one can write

$$\hat{H}_I = \frac{\epsilon}{4}\left(\hat{q}_\alpha - \hat{\mathsf{q}}_a\right)^2 + \frac{\epsilon}{4}\left(\hat{q}_\beta - \hat{\mathsf{q}}_b\right)^2. \tag{7}$$

As final remarks about the system Hamiltonian, note that in our notation, we have $\mathbf{H}_0 = \mathbf{H}_{\text{e}} \oplus \mathbf{H}_{\text{N}}$. Finally, given the forms of (6) and (7), the system Hamiltonian $\hat{H}$ is quadratic in $\hat{X}$, that is

$$\hat{H} = \tfrac{1}{2}\hat{X}^\dagger \mathbf{H} \hat{X}, \tag{8}$$

with $\mathbf{H}$ beeing the Hessian of $\hat{H}$. It is worth mentioning that, despite the specificity of the coupling Hamiltonian (7), both $\mathbf{H}_{\text{e}}$ and $\mathbf{H}_{\text{N}}$ in (6) are completely arbitrary until this point.

For the non-unitary part of (1), let us assume that every $\hat{L}_{(k)}$ in (2) is a linear function of position and momentum, *i.e.*,

$$\hat{L}_{(k)} = \lambda_{(k)}^\top \mathsf{J} \hat{X}, \tag{9}$$

where $\lambda_{(k)} \in \mathbb{C}^{2N+4}$ is a column vector and J the matrix defined in (5).

Of particular importance for continuous variable systems, one defines the covariance matrix (CM) of the system state as

$$\mathbf{V}_{jk}(t) = \tfrac{1}{2}\mathrm{Tr}\left[\left\{\hat{X}_j - \langle\hat{X}_j\rangle_t, \hat{X}_k - \langle\hat{X}_k\rangle_t\right\}\hat{\rho}(t)\right], \quad (10)$$

where $\hat{X}_j$ is the j^{th} component of $\hat{X}$ and $\langle\hat{X}_j\rangle_t := \mathrm{Tr}[\hat{X}_j\hat{\rho}(t)]$ is its mean value. Given its importance, we will be focusing on the time evolution of the CM in this paper.

With the help of (8) and (9), and by defining

$$\boldsymbol{\Upsilon} := \sum_k \lambda_{(k)}\lambda^\dagger_{(k)}, \quad (11)$$

it is possible to show that the CM equation of motion reads [16, 17]

$$\frac{d}{dt}\mathbf{V} = \boldsymbol{\Gamma}\mathbf{V} + \mathbf{V}\boldsymbol{\Gamma}^\top + \mathbf{D}, \quad (12)$$

with

$$\boldsymbol{\Gamma} := \mathsf{J}\mathbf{H} - \mathrm{Im}\boldsymbol{\Upsilon}\mathsf{J}, \quad \mathbf{D} := \hbar\,\mathrm{Re}\boldsymbol{\Upsilon}. \quad (13)$$

Since $\mathbf{H}$ and $\boldsymbol{\Upsilon}$ are *time independent*, the solution for (12) is

$$\mathbf{V}(t) = \mathrm{e}^{\boldsymbol{\Gamma}t}\,\mathbf{V}_0\,\mathrm{e}^{\boldsymbol{\Gamma}^\top t} + \int_0^t dt'\,\mathrm{e}^{\boldsymbol{\Gamma}t'}\,\mathbf{D}\,\mathrm{e}^{\boldsymbol{\Gamma}^\top t'}, \quad (14)$$

where $\mathbf{V}_0$ is the CM of the initial state.

As a final remark, for initial Gaussian states, the quadratic Hamiltonians and linear Lindbladians considered here will dynamically preserve Gaussian states and, for this case, the CM and the mean values embody all information about the system. However, even in cases where the initial state is not Gaussian, (14) is still correct. In such cases, the knowledge of the CM and of the mean values will not contain all information about the system state.

III. EFFECTIVE DYNAMICS

In this section, we will expand and generalize the results in [9] in order to treat arbitrary networks possessing a quadratic and positive definite Hamiltonian. Besides, we include the non-unitary contribution to the dynamics via a Lindblad equation. This last point adds interest to our generalizations due to the multitude of physical systems where dissipation can not be neglected in the description. The method consists in three steps. First, we diagonalize the free part of the system Hamiltonian. Then, we move the LME to an interaction picture where we can perform the RWA and a structural simplification to end up with an effective description for the dynamics of a, b, and a few normal modes of the network.

A. Symplectic Formalism

The development of our results is based on mathematical tools related to the symplectic formalism [16–20]. For the sake of simplicity, the basics will be illustrated using the N oscillators of the network, but everything is readily transposed to systems with an arbitrary number of members.

In this formalism, one is interested in transformations $\hat{x}' = \mathsf{S}\hat{x}$ of $\hat{x} = (\hat{q}_1, ..., \hat{q}_N, \hat{p}_1, ..., \hat{p}_N)^\dagger$ such that the transformed operators satisfy

$$[\hat{x}'_j, \hat{x}'_k] = i\hbar\,\mathsf{J}^{[N]}_{jk}. \quad (15)$$

One can show that this is guaranteed provided $\mathsf{S}^\top\mathsf{J}\mathsf{S} = \mathsf{J}$. The set of elements S satisfying such a statement forms the real symplectic group $\mathsf{S} \in \mathrm{Sp}(2N, \mathbb{R})$.

A central result for us here is the so called Williamson theorem [21]. It states that a positive definite $2N \times 2N$ symmetric matrix $\mathbf{M}$, *i.e.*, $\mathbf{M} = \mathbf{M}^\top > 0$, can be diagonalized by a symplectic congruence. In other words, there exists $\mathsf{S} \in \mathrm{Sp}(2N, \mathbb{R})$ such that

$$\mathsf{S}\mathbf{M}\mathsf{S}^\top = \Lambda_{\mathbf{M}}, \quad \Lambda_{\mathbf{M}} := \mathrm{Diag}(s_1, ..., s_N, s_1, ..., s_N) \quad (16)$$

with $0 < s_j \leq s_k$ for $j \leq k$. The double-paired ordered set (or the diagonal matrix) $\Lambda_{\mathbf{M}}$ is called *symplectic spectrum* of $\mathbf{M}$, and s_k are its symplectic eigenvalues (SE). These can also be found from the (Euclidean) eigenvalues of $\mathsf{J}\mathbf{M}$ [20], which turn out to be

$$\mathrm{Spec}_{\mathbb{C}}(\mathsf{J}\mathbf{M}) = \mathrm{Diag}(is_1, ..., is_N, -is_1, ..., -is_N). \quad (17)$$

The matrix S that diagonalizes $\mathbf{M}$ admits a suitable decomposition as

$$\mathsf{S} = \Lambda_{\mathbf{M}}^{\frac{1}{2}} O \mathbf{M}^{-\frac{1}{2}} \quad (18)$$

with $O \in \mathrm{O}(2N)$, *i.e.*, an orthogonal matrix. From the symplectic condition on S, one can see that O must obey

$$O\mathbf{M}^{\frac{1}{2}}\mathsf{J}\mathbf{M}^{\frac{1}{2}}O^\top = \Lambda_{\mathbf{M}}\mathsf{J}. \quad (19)$$

If convenient, one can equivalently use creation/annihilation operators instead of position and momentum. In this case, one can define the column vector

$$\hat{z} := (\hat{a}^\dagger_1, ..., \hat{a}^\dagger_N, -i\hat{a}_1, ..., -i\hat{a}_N)^\dagger, \quad (20)$$

where $\hat{a}_k := (\hat{q}_k + i\hat{p}_k)/\sqrt{2\hbar}$ is the annihilation operator. This change of coordinates can be compactly represented by

$$\sqrt{\hbar}\,\hat{z} = \mathsf{C}_{[N]}\hat{x} \quad (21)$$

with

$$\mathsf{C}_{[n]} := \frac{1}{\sqrt{2}}\begin{pmatrix} \mathsf{I}_n & i\mathsf{I}_n \\ i\mathsf{I}_n & \mathsf{I}_n \end{pmatrix}, \quad \mathsf{C}^\dagger_{[n]} = \mathsf{C}^{-1}_{[n]}. \quad (22)$$

One can show that $\mathsf{C}_{[n]}$ is symplectic, and this leads immediately to

$$[\hat{z}_j, \hat{z}_k] = i\,\mathsf{J}^{[N]}_{jk}. \quad (23)$$

If clear in context, the sub- or superscript $[n]$ will be omitted.

Giving S as defined in (18), one may wonder which conditions should be imposed to $\mathbf{M}$ in order to make $\mathsf{S}\mathsf{S}^\top$ diagonal. To answer this question, let us define the diagonal matrix $\mathsf{L} := \boldsymbol{L} \oplus \boldsymbol{L}^{-1} \in \mathrm{Sp}(2N, \mathbb{R})$, where $\boldsymbol{L} := \mathrm{Diag}(l_1, ..., l_N)$ with $l_i > 0 \forall i$. According to *theorem 5* in [25], there exists a symplectic rotation $\mathsf{R} \in \mathrm{Sp}(2N, \mathbb{R}) \cap \mathrm{O}(2N)$ such that

$$\mathsf{R}\mathbf{M}\mathsf{R}^\top = \mathsf{L}\,\Lambda_{\mathbf{M}}\,\mathsf{L}^\top, \tag{24}$$

if and only if

$$\begin{aligned} &[\mathbf{M_Q}, \mathbf{M_P}] = \mathbf{M_C}^2 - \mathbf{M_C}^{\top 2}, \\ &\mathbf{M_P}\mathbf{M_C} - \mathbf{M_C}^\top\mathbf{M_P} = \mathbf{M_C}\mathbf{M_Q} - \mathbf{M_Q}\mathbf{M_C}^\top, \end{aligned} \tag{25}$$

where we wrote $\mathbf{M}$ in terms of $N \times N$ blocks, *i.e.*,

$$\mathbf{M} = \begin{pmatrix} \mathbf{M_Q} & \mathbf{M_C} \\ \mathbf{M_C}^\top & \mathbf{M_P} \end{pmatrix}. \tag{26}$$

Once conditions (25) are fulfilled, the choice $\mathsf{S} := \mathsf{L}^{-1}\mathsf{R}$ leads to $\mathsf{S}\mathbf{M}\mathsf{S}^\top = \Lambda_{\mathbf{M}}$, as a direct consequence of (24). In this way,

$$\mathsf{S}\mathsf{S}^\top = \mathsf{L}^{-1}\mathsf{R}(\mathsf{L}^{-1}\mathsf{R})^\top = \mathsf{L}^{-2} = \boldsymbol{L}^{-2} \oplus \boldsymbol{L}^2 \tag{27}$$

which is a diagonal matrix giving the way $\boldsymbol{L}$ was defined.

B. Diagonalization of $\hat{H}_0$

We now require the matrix $\mathbf{H}_0$ appearing in (6) to be positive definite, and this is the only restriction imposed on the network of Fig. 1. On the basis of the Williamson theorem, we know that there is a symplectic matrix $\mathsf{S}_0 = \mathsf{S}_\mathrm{e} \oplus \mathsf{S}_\mathrm{N}$ such that

$$\mathsf{S}_0\mathbf{H}_0\mathsf{S}_0^\top = \Lambda_\mathrm{e} \oplus \Lambda_\mathrm{N}, \tag{28}$$

where

$$\Lambda_\mathrm{N} := \mathrm{Diag}(\varsigma_1, ..., \varsigma_N, \varsigma_1, ..., \varsigma_N) \tag{29}$$

is the symplectic spectrum of $\mathbf{H}_\mathrm{N}$.

For the external oscillators, we may particularize to the case where they are identical with natural frequencies Ω and masses M. In this case, their contribution to the Hamiltonian in (6) is given by

$$\mathbf{H}_\mathrm{e} = M\Omega^2\,\mathsf{I}_2 \oplus M^{-1}\mathsf{I}_2, \tag{30}$$

with symplectic spectrum $\Lambda_\mathrm{e} = \Omega\mathsf{I}_4$. One interesting situation arises when "$M\Omega = 1$" in a given system of units, for example, kilogram times radian. One can see that, in this case, Hamiltonian (30) will be directly expressed in terms of normal mode coordinates with doubly degenerate frequency Ω.

The normal modes $\hat{Y} := (\hat{\mathsf{y}}^\dagger, \hat{y}^\dagger)^\dagger$ for the whole system, by definition, relates to the original coordinates through

$$\hat{X} = \mathsf{S}_0^\top\hat{Y} = \begin{pmatrix} \mathsf{S}_\mathrm{e}^\top\hat{\mathsf{y}} \\ \mathsf{S}_\mathrm{N}^\top\hat{y} \end{pmatrix}, \tag{31}$$

where S_0 is the symplectic transformation that diagonalizes the Hessian $\mathbf{H}_0$ in (28). In terms of creation/annihilation operators,

$$\sqrt{\hbar}\,\hat{Z} = \left(\mathsf{C}_{[2]} \oplus \mathsf{C}_{[N]}\right)\hat{Y}, \tag{32}$$

which implies by (31) that

$$\hat{X} = \sqrt{\hbar}\,\left(\mathsf{S}_\mathrm{e}^\top\mathsf{C}_{[2]}^\dagger \oplus \mathsf{S}_\mathrm{N}^\top\mathsf{C}_{[N]}^\dagger\right)\hat{Z}, \tag{33}$$

with $\hat{Z} = (\hat{\mathsf{z}}^\dagger, \hat{z}^\dagger)^\dagger$. Finally, using the transformation (33) in the free Hamiltonian (6), one finds

$$\hat{H}_0 = \frac{\hbar}{2}\,\hat{Z}^\dagger(\Lambda_\mathrm{e} \oplus \Lambda_\mathrm{N})\hat{Z} = \frac{\hbar\Omega}{2}\,\hat{\mathsf{z}}^\dagger\hat{\mathsf{z}} + \frac{\hbar}{2}\,\hat{z}^\dagger\Lambda_\mathrm{N}\hat{z}, \tag{34}$$

which is the free Hamiltonian (6) written in the creation/annihilation representation of the normal mode coordinates.

C. Interaction Picture

Let us now move the dynamics to the interaction picture with respect to the free Hamiltonian as given in Eq. (34). The LME in this picture acquires the following form

$$\frac{d\tilde{\rho}}{dt} = \frac{i}{\hbar}[\tilde{\rho}, \tilde{H}] + \tilde{\mathcal{L}}(\tilde{\rho}), \tag{35}$$

with $\tilde{H} = \mathrm{e}^{\frac{i}{\hbar}\hat{H}_0 t}\,\hat{H}\,\mathrm{e}^{-\frac{i}{\hbar}\hat{H}_0 t} - \hat{H}_0$ and $\tilde{\rho} = \mathrm{e}^{\frac{i}{\hbar}\hat{H}_0 t}\,\hat{\rho}\,\mathrm{e}^{-\frac{i}{\hbar}\hat{H}_0 t}$. Also, all operators contained in $\mathcal{L}$ transform in the same way as $\hat{\rho}$, leading then to $\tilde{\mathcal{L}}(\tilde{\rho})$. By now, let us turn our attention to the Hamiltonian part.

When moving to the interaction picture, the position operators of the oscillators in the chain and of the external ones, see (33), transform respectively according to

$$\begin{aligned} &\tilde{q}_k = \tilde{x}_k = \sqrt{\hbar}\left(\mathsf{S}_\mathrm{N}^\top\mathsf{C}_{[N]}^\dagger\tilde{z}\right)_k, \;\; 1 \geq k \geq N; \\ &\tilde{\mathsf{q}}_k = \tilde{\mathsf{x}}_k = \sqrt{\frac{\hbar}{2}}(\tilde{\mathsf{a}}_k + \tilde{\mathsf{a}}_k^\dagger), \;\; k = a, b. \end{aligned} \tag{36}$$

For what comes next, it is worth noticing that

$$\tilde{q}_k^2 = \tilde{x}_k^2 = (\tilde{x}\tilde{x}^\dagger)_{kk} = \hbar\left(\mathsf{S}_\mathrm{N}^\top\mathsf{C}_{[N]}^\dagger\tilde{z}\tilde{z}^\dagger\mathsf{S}_\mathrm{N}^\top\mathsf{C}_{[N]}^\dagger\right)_{kk}. \tag{37}$$

Now, with all these in hand, we move $\hat{H} = \hat{H}_0 + \hat{H}_I$ to the interaction picture. By using (7) and (34), one can see that the interaction picture Hamiltonian reads

$$\begin{aligned} \tilde{H} &= \frac{\epsilon}{4}(\tilde{q}_\alpha - \tilde{q}_a)^2 + \frac{\epsilon}{4}(\tilde{q}_\beta - \tilde{q}_b)^2 \\ &= \frac{\hbar\epsilon}{4}\left[\left(\mathsf{S}^\top\mathsf{C}^\dagger\tilde{z}\tilde{z}^\dagger\mathsf{C}\mathsf{S}\right)_{\alpha\alpha} + \left(\mathsf{S}^\top\mathsf{C}^\dagger\tilde{z}\tilde{z}^\dagger\mathsf{C}\mathsf{S}\right)_{\beta\beta}\right] \\ &- \frac{\hbar\epsilon}{2\sqrt{2}}\left[\left(\mathsf{S}^\top\mathsf{C}^\dagger\tilde{z}\right)_\alpha(\tilde{\mathsf{a}}_a + \tilde{\mathsf{a}}_a^\dagger) + \left(\mathsf{S}^\top\mathsf{C}^\dagger\tilde{z}\right)_\beta(\tilde{\mathsf{a}}_b + \tilde{\mathsf{a}}_b^\dagger)\right] \\ &+ \frac{\hbar\epsilon}{8}(\tilde{\mathsf{a}}_a + \tilde{\mathsf{a}}_a^\dagger)^2 + \frac{\hbar\epsilon}{8}(\tilde{\mathsf{a}}_b + \tilde{\mathsf{a}}_b^\dagger)^2, \end{aligned} \tag{38}$$

where we dropped the indexes of $\mathsf{S}_{\rm N}$ and of $\mathsf{C}_{[N]}$ for notation simplicity, and

$$\begin{aligned}\tilde{z}_k &:= \mathrm{e}^{\frac{i}{\hbar}\hat{H}_0 t}\,\hat{z}_k\,\mathrm{e}^{-\frac{i}{\hbar}\hat{H}_0 t} = \mathrm{e}^{i\phi_k t}\hat{z}_k \;\; (k=1,...,2N),\\ \tilde{\mathsf{a}}_k &:= \mathrm{e}^{-i\Omega t}\hat{\mathsf{a}}_k \;\; (k=a,b),\end{aligned} \tag{39}$$

with

$$\phi_k := \begin{cases} -\varsigma_k, & \text{if } k\le N \\ \varsigma_{k-N}, & \text{if } k>N \end{cases}. \tag{40}$$

Notice that $\tilde{z}_k$ is $\tilde{a}_k = \hat{a}_k \mathrm{e}^{-i\varsigma_k t}$ provided $k \le N$ or its hermitian conjugate otherwise.

D. RWA and Effective Hamiltonian

Under certain circumstances, fast oscillating terms in the interaction picture Hamiltonian are negligible and dropping these terms is what is called RWA. In the Appendix A, we quantitatively describe such conditions for a prototype system of two coupled oscillators. This guides us in the application of the RWA for the present system of interest.

Since the free Hamiltonian (34) is the sum of $N+2$ non-interacting oscillators, each of its eigenvectors consists of tensor products of Fock states of each oscillator, *i.e.*,

$$|\Psi\rangle = |\mathfrak{n}_a, \mathfrak{n}_b, \mathfrak{n}_1, ..., \mathfrak{n}_N\rangle, \tag{41}$$

where $\{|\mathfrak{n}_k\rangle; k = 1,...,N\}$ are eigenstates of $\hat{a}_k^\dagger \hat{a}_k$ and $\{|\mathfrak{n}_k\rangle; k = a,b\}$, the eigenstates of $\hat{\mathsf{a}}_k^\dagger \hat{\mathsf{a}}_k$. All transitions between eigenstates of the free Hamiltonian will be promoted by $\tilde{H}_I$, *i.e.*, by (38). Allowed transitions $|\Psi'\rangle \leftrightarrow |\Psi\rangle$, in the scope of first order perturbation theory, are those with $\langle\Psi|\tilde{H}_I|\Psi'\rangle \neq 0$. First-order time-dependent perturbation theory [22] predicts that resonant or quasi-resonant transitions or, equivalently, those driven by static or slowly varying time dependent terms in the interaction picture Hamiltonian, take place with higher probability when compared to transitions driven by the rapidly oscillating terms. The RWA consists of discarding the highly oscillating terms in the interaction Hamiltonian that are responsible for negligible transition amplitudes when compared to other terms that are static or oscillate slowly in time. Appendix A is dedicated to considerations about this approximation. Since the reasoning for usefulness of the RWA is that of the first-order perturbation theory, we must assure that H_I is weak compared to H_0. In our problem, this means that the interaction of the external oscillators with the network is weak, and this is guaranteed provided $\epsilon \ll \Omega, \varsigma_k$ $(k = 1,...,N)$.

Let us start with the case where the spectrum (29) is *non-degenerate*. Mathematically, that corresponds to $\varsigma_j = \varsigma_k$ if and only if $j = k$. In the system considered here, a interesting scenario appears when the frequency of the external oscillators Ω is close to the frequency of one of the normal modes of the network, let us say the $m^{\rm th}$ mode $(1 \le m \le N)$, *i.e.*, $\Omega = \varsigma_m$. In this case, if (39) is substituted in (38), the RWA can be performed using the recipe

$$\begin{aligned}&\tilde{z}_k\tilde{z}_l^\dagger = \hat{z}_k\hat{z}_l^\dagger\,\mathrm{e}^{i(\phi_k-\phi_l)t} \xrightarrow{\text{RWA}} \hat{z}_k\hat{z}_l^\dagger\,\delta_{kl},\\ &\tilde{\mathsf{a}}_l^2 = \hat{\mathsf{a}}_l^2\mathrm{e}^{-2i\Omega t} \xrightarrow{\text{RWA}} 0,\;\; \tilde{\mathsf{a}}_l^{\dagger 2} = \hat{\mathsf{a}}_l^{\dagger 2}\mathrm{e}^{2i\Omega t} \xrightarrow{\text{RWA}} 0,\\ &\tilde{z}_k\tilde{\mathsf{a}}_l^\dagger = \hat{z}_k\hat{\mathsf{a}}_l^\dagger\,\mathrm{e}^{i(\phi_k+\Omega)t} \xrightarrow{\text{RWA}} \hat{z}_k\hat{\mathsf{a}}_l^\dagger\,\delta_{km},\\ &\tilde{z}_k\tilde{\mathsf{a}}_l = \hat{z}_k\hat{\mathsf{a}}_l\,\mathrm{e}^{i(\phi_k-\Omega)t} \xrightarrow{\text{RWA}} \hat{z}_k\hat{\mathsf{a}}_l\,\delta_{k\,m+N}.\end{aligned} \tag{42}$$

One can see that, under resonance condition $\Omega = \varsigma_m$ and weak interaction of external oscillators with the network, both necessary conditions for RWA to work well, oscillators a and b couple essentially only with the $m^{\rm th}$ normal mode. Since modes other than m follow free evolution, we do not include them in the effective description of the dynamics. Taking all these in to account, we can arrive at the following effective Hamiltonian[1]

$$\begin{aligned}\tilde{H}_{\rm eff}^{(m)} &= \frac{\hbar\epsilon}{4}\mathcal{C}_m^{\alpha\beta}\hat{a}_m^\dagger\hat{a}_m + \frac{\hbar\epsilon}{4}(\hat{\mathsf{a}}_a^\dagger\hat{\mathsf{a}}_a + \hat{\mathsf{a}}_b^\dagger\hat{\mathsf{a}}_b)\\ &\quad - \frac{\hbar\epsilon}{4}\left[\mathcal{D}_m^\alpha\hat{a}_m\hat{\mathsf{a}}_a^\dagger + \bar{\mathcal{D}}_m^\alpha\hat{a}_m^\dagger\hat{\mathsf{a}}_a + \mathcal{D}_m^\beta\hat{a}_m\hat{\mathsf{a}}_b^\dagger + \bar{\mathcal{D}}_m^\beta\hat{a}_m^\dagger\hat{\mathsf{a}}_b\right],\end{aligned} \tag{43}$$

with

$$\begin{aligned}\mathcal{C}_m^{\alpha\beta} &:= (\mathsf{S}_{m\alpha}^2 + \mathsf{S}_{m+N\alpha}^2 + \mathsf{S}_{m\beta}^2 + \mathsf{S}_{m+N\beta}^2),\\ \mathcal{D}_m^\mu &:= (\mathsf{S}_{m\mu} - i\mathsf{S}_{m+N\,\mu}),\;\; \bar{\mathcal{D}}_m^\mu := (\mathsf{S}_{m\mu} + i\mathsf{S}_{m+N\,\mu}).\end{aligned} \tag{44}$$

If the symplectic spectrum possess some degree of degeneracy, let us say $\varsigma_m = \varsigma_n$ for some $1 \le n, m \le N$, and we tune $\Omega = \varsigma_m = \varsigma_n$, then scheme (42) is no longer valid. It must be modified to

$$\begin{aligned}&\tilde{z}_k\tilde{z}_l^\dagger \xrightarrow{\text{RWA}} \hat{z}_k\hat{z}_l^\dagger\,(\delta_{kl} + \delta_{km}\delta_{ln} + \delta_{kn}\delta_{lm} +\\ &\qquad\qquad \delta_{k\,m+N}\,\delta_{l\,n+N} + \delta_{k\,n+N}\,\delta_{l\,m+N}),\\ &\tilde{\mathsf{a}}_l^2 = \hat{\mathsf{a}}_l^2\mathrm{e}^{-2i\Omega t} \xrightarrow{\text{RWA}} 0,\;\; \tilde{\mathsf{a}}_l^{\dagger 2} = \hat{\mathsf{a}}_l^{\dagger 2}\mathrm{e}^{2i\Omega t} \xrightarrow{\text{RWA}} 0,\\ &\tilde{z}_k\tilde{\mathsf{a}}_l^\dagger \xrightarrow{\text{RWA}} \hat{z}_k\hat{\mathsf{a}}_l^\dagger\,(\delta_{km} + \delta_{kn}),\\ &\tilde{z}_k\tilde{\mathsf{a}}_l \xrightarrow{\text{RWA}} \hat{z}_k\hat{\mathsf{a}}_l\,(\delta_{k\,m+N} + \delta_{k\,n+N}).\end{aligned} \tag{45}$$

The additional terms, in comparison with (42), bring new elements for the dynamics the system. Now, the situation involves the free dynamics of the degenerate modes, their mutual coupling, and their coupling with the external oscillators. Following the same steps as before, we can now write an effective Hamiltonian for the system as

$$\begin{aligned}\tilde{H}_{\rm eff}^{(m,n)} &= \tilde{H}_{\rm eff}^{(m)} + \tilde{H}_{\rm eff}^{(n)} - \frac{\hbar\epsilon}{4}(\hat{\mathsf{a}}_a^\dagger\hat{\mathsf{a}}_a + \hat{\mathsf{a}}_b^\dagger\hat{\mathsf{a}}_b)\\ &+ \frac{\hbar\epsilon}{4}(\mathsf{S}_{m\alpha}\mathsf{S}_{n\alpha} + \mathsf{S}_{m+N\alpha}\mathsf{S}_{n+N\alpha})(\hat{a}_m^\dagger\hat{a}_n + \hat{a}_n^\dagger\hat{a}_m)\\ &+ \frac{\hbar\epsilon}{4}(\mathsf{S}_{m\beta}\mathsf{S}_{n\beta} + \mathsf{S}_{m+N\beta}\mathsf{S}_{n+N\beta})(\hat{a}_m^\dagger\hat{a}_n + \hat{a}_n^\dagger\hat{a}_m)\\ &+ i\frac{\hbar\epsilon}{4}(\mathsf{S}_{m\alpha}\mathsf{S}_{n+N\alpha} - \mathsf{S}_{m+N\alpha}\mathsf{S}_{n\alpha})(\hat{a}_m^\dagger\hat{a}_n - \hat{a}_n^\dagger\hat{a}_m)\\ &+ i\frac{\hbar\epsilon}{4}(\mathsf{S}_{m\beta}\mathsf{S}_{n+N\beta} - \mathsf{S}_{m+N\beta}\mathsf{S}_{n\beta})(\hat{a}_m^\dagger\hat{a}_n - \hat{a}_n^\dagger\hat{a}_m),\end{aligned} \tag{46}$$

[1] It can be useful to write the elements of $\mathsf{C}_{[n]}$ in (22) as $(\delta_{jk} + i\delta_{jk+n} + i\delta_{jk-n})/\sqrt{2}$.

where $\tilde{H}_{\rm eff}^{(k)}$ is given in (43) for $k = m, n$.

One may notice that, if $\mathsf{S}_{m\alpha} = \mathsf{S}_{m+N\alpha} = 0$ in (43) or in (46), oscillator a will be decoupled from the $m^{\rm th}$ normal mode of the network. Physically, position α would correspond to a *node* of the normal mode. In this situation, the coupling of the external oscillator a with the normal mode m takes place only for higher orders in ϵ. Naturally, there is an analogous conditions for oscillator b.

For completeness, we would also like to mention the possibility of the external oscillators interacting with more than one member of the network. Suppose that oscillator b is coupled to both oscillators β and β' simultaneously, *i.e.*, the interaction Hamiltonian is now

$$\hat{H}_I' = \hat{H}_I + \frac{\epsilon'}{4}\left(\hat{q}_{\beta'} - \hat{\mathsf{q}}_b\right)^2 \tag{47}$$

with $\hat{H}_I$ given in (7). All the calculations follow as before provided one now imposes $\epsilon' \ll \Omega$, in order to fulfill the RWA requirements. Specially, we would like to emphasize that S_0 defined above Eq. (28) remains the same. After the calculations, the result is

$$\begin{aligned}\tilde{H}_{\rm eff}^{'(m)} = \tilde{H}_{\rm eff}^{(m)} + \frac{\hbar\epsilon'}{4}\mathcal{E}_m^{\beta'}\hat{a}_m^\dagger\hat{a}_m + \frac{\hbar\epsilon'}{4}\hat{\mathsf{a}}_b^\dagger\hat{\mathsf{a}}_b \\ - \frac{\hbar\epsilon'}{4}\left[\mathcal{D}_m^{\beta'}\hat{a}_m\hat{\mathsf{a}}_b^\dagger + \bar{\mathcal{D}}_m^{\beta'}\hat{a}_m^\dagger\hat{\mathsf{a}}_b\right],\end{aligned} \tag{48}$$

with $\tilde{H}_{\rm eff}^{(m)}$ in (43), $\mathcal{D}_m^{\beta'}$ in (44), and $\mathcal{E}_m^{\beta'} := \mathsf{S}_{m\beta'}^2 + \mathsf{S}_{m+N\beta'}^2$. Note also that if one wants to consider in (7) the possibility of distinct couplings namely ϵ for (a,α) and ϵ' for (b,β), the use of (48) for the part referring to (b,β) is the way to proceed.

E. Thermal Baths and Effective Dynamics

The unavoidable incapacity of a perfect system isolation leads to the progressive destruction of quantum coherence. This kind of dynamics is commonly modeled by including appropriate non-unitary components in the equation of motion. We will specialize here in the case of local and independent thermal baths for each member of the system depicted in Fig.1. This physical scenario corresponds to the use of (2) with the choice

$$\begin{aligned}\hat{L}_{(k)} &= \sqrt{\hbar\zeta(\bar{n}_{\rm th}+1)}\,\hat{A}_k, \\ \hat{L}'_{(k)} &= \sqrt{\hbar\zeta\bar{n}_{\rm th}}\,\hat{A}_k^\dagger, \quad (k = a, b, 1, 2, ..., N),\end{aligned} \tag{49}$$

where $\hat{A}_k$ is the annihilation operator associated to the $k^{\rm th}$ component of $\hat{X}$, $\zeta \geq 0$ is the effective bath-oscillator coupling constant or relaxation rate of the system, and $\bar{n}_{\rm th}$ is a thermal occupation number, both taken here to be the same for all reservoirs. Note that, for the same k, two Lindblad operators must be simultaneously included (primed and unprimed). The prescribed Lindblad operators do not couple different oscillators, and this brings the matrix (11) to a block structure

$$\boldsymbol{\Upsilon} = \boldsymbol{\Upsilon}_4 \oplus \boldsymbol{\Upsilon}_{2N}, \tag{50}$$

with

$$\boldsymbol{\Upsilon}_{2n} := \zeta(\bar{n}_{\rm th} + \tfrac{1}{2})\mathsf{I}_n - \frac{i}{2}\zeta\mathsf{J}^{[n]}, \tag{51}$$

where n equals 2 or N.

Now, the same transformation (31), used to diagonalize $\hat{H}_0$ in (28), must be applied to the Lindblad operators defined in (9). Consequently,

$$\hat{L}_{(k)} = \lambda_{(k)}^\top\mathsf{J}\mathsf{S}_0^\top\hat{Y} = [\mathsf{S}_0^{-\top}\lambda_{(k)}]^\top\mathsf{J}\hat{Y}. \tag{52}$$

To see that, one must apply the sympleticity of S_0, *i.e.*, $\mathsf{S}_0^\top\mathsf{J}\mathsf{S}_0 = \mathsf{J}$. Notice that we used a compact notation $\mathsf{S}_0^{-\top}$ for $(\mathsf{S}_0^\top)^{-1}$. Given (11), we see that

$$\boldsymbol{\Upsilon} \longrightarrow \mathsf{S}_0^{-\top}\boldsymbol{\Upsilon}\mathsf{S}_0^{-1}, \tag{53}$$

in such a way that (50) becomes

$$\mathsf{S}_0^{-\top}\boldsymbol{\Upsilon}\mathsf{S}_0^{-1} = \zeta(\bar{n}_{\rm th}+\tfrac{1}{2})(\mathsf{S}_0\mathsf{S}_0^\top)^{-1} - \tfrac{i}{2}\zeta\left(\mathsf{J}^{[2]}\oplus\mathsf{J}^{[N]}\right), \tag{54}$$

where we used the symplecticity of S_0 again.

Our aim is to provide the simplest description of the dynamics of oscillators a and b mediated by the network. At the Hamiltonian level, we already managed to do that when we arrived at an effective interaction involving just these oscillators and a few resonant normal modes. For the Lindblad operators and covariance matrices, the description in terms of normal modes is reflected in (54). In general, the normal modes turn out to be interacting in spite of the fact that, looking at the individual oscillators, they interact with independent baths. One can say that the action of the baths, in the level of normal modes (which are collective operators), is non-local. The interaction of the normal modes in the non-unitary part of the dynamics comes from the mutual interactions of the individual oscillators in the Hamiltonian, *i.e.*, in the unitary part of the dynamics. Consequently, (54) might not be as simple as (51), remembering that the latter refers to a description of local independent baths. From this, we see that the problem of obtaining a simple description of the open system dynamics is much more involved than the same problem in the closed unitary dynamics. So, together with the treatment of a general network, the possible simplifications for the open system dynamics we do next make our contribution of interest giving that previous studies treated only closed systems in a fixed simple topology [9].

It is possible to envision some structural conditions that make (54) simpler. In other words, conditions that lead to local and independent baths for the collective normal modes. This basically concerns the form of the matrix $\mathsf{S}_0\mathsf{S}_0^\top$ (topology), or the form of $\lambda_{(k)}$ (system-bath interaction). Let us start with the first condition which will be illustrated with an example in Sec. IV.

Direct inspection of (54) reveals that the baths for the normal modes will naturally be local and independent provided $\mathsf{S}_0\mathsf{S}_0^\top$ becomes a diagonal matrix. One possibility is $\mathsf{S}_0\mathsf{S}_0^\top = \mathsf{I}_4 \oplus \mathsf{I}_{2N}$ what would lead precisely to a form like (51), corresponding to interaction with local independent baths. When $\mathsf{S}_0\mathsf{S}_0^\top$ is diagonal but not the identity matrix, each mode will

still see a local reservoir but it will not necessarily be thermal. In this case there is a weighted mix of creation and annihilation operators characteristic of a squeezed reservoir. Given the quadratic Hamiltonian in (6), the results in Sec.III A will be helpful to determine if the action of the reservoirs will be decoupled or not. Provided the blocks of $\mathbf{H}_{\rm N}$ satisfy the conditions in (25), it will be suitable for symplectic diagonalization by a matrix $\mathsf{S}_{\rm N}$ such that $\mathsf{S}_{\rm N}\mathsf{S}_{\rm N}^{\top}$ is a diagonal matrix. Considering that the same is true for the blocks of $\mathbf{H}_{\rm e}$ in (6), then S_0 in (28) will be such that $\mathsf{S}_0\mathsf{S}_0^{\top}$ is diagonal.

For resonance of a and b with a non-degenerate normal mode m, we define

$$\check{x} = (\hat{\mathsf{q}}_a, \hat{\mathsf{q}}_b, \hat{y}_m, \hat{\mathsf{p}}_a, \hat{\mathsf{p}}_b, \hat{y}_{m+N})^{\dagger}, \tag{55}$$

from which we may write the effective Hamiltonian (43) as

$$\hat{H}_{\rm eff}^{(m)} = \frac{1}{2}\check{x}^{\dagger}\mathbf{H}_{\rm eff}\check{x} = \frac{\epsilon}{8}\check{x}^{\dagger}\begin{pmatrix}\mathbf{H}_{\mathbf{q}} & \mathbf{C}_{\mathbf{qp}}\\ \mathbf{C}_{\mathbf{qp}}^{\top} & \mathbf{H}_{\mathbf{p}}\end{pmatrix}\check{x} \tag{56}$$

with

$$\mathbf{H}_{\mathbf{q}} = \mathbf{H}_{\mathbf{p}} = \begin{bmatrix} 1 & 0 & -\mathsf{S}_{m\alpha} \\ 0 & 1 & -\mathsf{S}_{m\beta} \\ -\mathsf{S}_{m\alpha} & -\mathsf{S}_{m\beta} & (\mathsf{S}^2_{m\alpha}+\mathsf{S}^2_{m\beta}+ \\ & & \mathsf{S}^2_{m+N\,\alpha}+\mathsf{S}^2_{m+N\,\beta}) \end{bmatrix}, \tag{57}$$

and

$$\mathbf{C}_{\mathbf{qp}} = \begin{bmatrix} 0 & 0 & -\mathsf{S}_{m+N\,\alpha} \\ 0 & 0 & -\mathsf{S}_{m+N\,\beta} \\ \mathsf{S}_{m+N\,\alpha} & \mathsf{S}_{m+N\,\beta} & 0 \end{bmatrix}. \tag{58}$$

Using (10), a CM based on $\check{x}$ can be built and, just like (12), it will evolve according to

$$\frac{d}{dt}\check{\mathbf{V}} = \check{\mathbf{\Gamma}}\check{\mathbf{V}} + \check{\mathbf{V}}\check{\mathbf{\Gamma}}^{\top} + \check{\mathbf{D}} \tag{59}$$

with

$$\check{\mathbf{\Gamma}} := \mathsf{J}^{[6]}\mathbf{H}_{\rm eff} - \frac{\zeta}{2}\mathsf{I}_6, \quad \check{\mathbf{D}} := \hbar\zeta(\bar{n}_{\rm th}+\tfrac{1}{2})\mathsf{D}, \tag{60}$$

where D will be a 6×6 diagonal matrix since $\mathsf{S}_0\mathsf{S}_0^{\top}$ is considered to be diagonal. Solution (14) applied to this effective description reads

$$\check{\mathbf{V}}(t) = \mathrm{e}^{\check{\mathbf{\Gamma}}t}\,\check{\mathbf{V}}_0\,\mathrm{e}^{\check{\mathbf{\Gamma}}^{\top}t} + \int_0^t dt'\,\mathrm{e}^{\check{\mathbf{\Gamma}}t'}\,\check{\mathbf{D}}\,\mathrm{e}^{\check{\mathbf{\Gamma}}^{\top}t'}, \tag{61}$$

with $\exp[\check{\mathbf{\Gamma}}t] = \mathrm{e}^{-\zeta t/2}\mathsf{E}(t)$, where

$$\mathsf{E}(t) = \exp\left[\mathsf{J}\mathbf{H}_{\rm eff}\,t\right] \in \mathrm{Sp}(6,\mathbb{R}). \tag{62}$$

This represents a huge simplification to the original problem which is to describe the open system dynamics of a and b when they interact with a network of N oscillators. This is especially true for big networks.

For a *degenerate* mode frequency, it suffices to build a vector just like (55) but now containing all the degenerate modes. From this, one can proceed as in the non-degenerate case. For example, if the symplectic eigenvalue is two-fold degenerate, say modes m and n, we define

$$\check{x} = (\hat{\mathsf{q}}_a, \hat{\mathsf{q}}_b, \hat{y}_m, \hat{y}_n, \hat{\mathsf{p}}_a, \hat{\mathsf{p}}_b, \hat{y}_{m+N}, \hat{y}_{n+N})^{\dagger}, \tag{63}$$

and $\mathbf{H}_{\rm eff}$, $\check{\mathbf{\Gamma}}$ and $\check{\mathbf{D}}$ will be 8×8 matrices. An example will be given in Sec.V B.

Let us now present a second condition allowing the description of the normal modes as subjected to local and non-interacting baths. This will happen whenever $\lambda_{(k)}$ appearing in (9) is of the special form $\lambda_{(k)} = \mathsf{S}_0^{\top}\mu_{(k)}$, where S_0 is the symplectic matrix diagonalizing the Hamiltonian (28), and $\mu_{(k)}$ corresponds to local thermal baths. In other words, μ_k is determined from $\hat{L}_k = \mu_{(k)}^{\top}\mathsf{J}\hat{X}$ with $\hat{L}_k$ given by (49). Under these circumstances, the transformed matrix $\mathsf{S}_0^{-\top}\mathbf{\Upsilon}\mathsf{S}_0^{-1}$ in (53) assumes the form (50) as a direct consequence of the symplectic property of S_0:

$$\hat{L}_k = \lambda_{(k)}^{\top}\mathsf{J}\hat{X} = (\mathsf{S}_0^{\top}\mu_{(k)})^{\top}\mathsf{J}\mathsf{S}_0^{\top}\hat{Y} = \mu_{(k)}^{\top}\mathsf{J}\hat{Y}. \tag{64}$$

Since $\mu_{(k)}$ corresponds to local thermal baths, we achieved our goal.

If we give up the requirement of having local baths, there is still other possibilities to attain an effective LME involving just a few degrees of freedom. For instance, when the structure of the network is such that the transformed Υ in (54) only interconnects the resonant oscillators, the effective dynamics will still only involve themselves, but possibly in a non-local way.

IV. EXAMPLE: LINEAR CHAIN

Consider a chain of N harmonic oscillators with frequency ω and coupled by springs (Hooke's law) with coupling constant κ, as depicted in Fig.2. The external oscillators a and b couples respectively with the $\alpha^{\rm th}$ and $\beta^{\rm th}$ oscillators of the chain as in (7) and have frequency Ω.

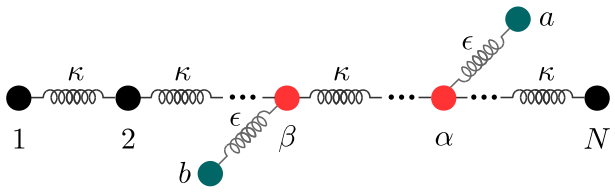


Figure 2. Chain of N-coupled harmonic oscillators as a network where oscillators a and b are attached at positions α and β, respectively. Coupling constants κ and ϵ refer to Hooke-like forces.

The free Hamiltonian (6) for this particular configuration is defined with

$$\mathbf{H}_{\rm e} = \Omega\mathsf{I}_4, \quad \mathbf{H}_{\rm N} = \mathbf{Q}\oplus\omega\,\mathsf{I}_N, \tag{65}$$

where $\mathbf{Q}$ is a $N\times N$ potential matrix whose elements are given by

$$\mathbf{Q}_{jk} = (\omega+\kappa)\delta_{jk} - \tfrac{\kappa}{2}(\delta_{j1}\delta_{1k} + \delta_{jn}\delta_{nk} + \delta_{jk\pm 1}). \tag{66}$$

Notice that we are taking $M\Omega = 1$ as discussed in Sec.III B.

The matrix $\mathbf{Q}$ in (66) is tridiagonal and symmetric what implies that it can be diagonalized by an orthogonal transformation [23]. In particular, $\boldsymbol{O}\mathbf{Q}\boldsymbol{O}^{\top} = \mathrm{Diag}(h_1, ..., h_N)$, with

$$\begin{aligned} \boldsymbol{O}_{jk} &= \sqrt{\frac{2-\delta_{j1}}{N}}\,\cos\tfrac{(j-1)(2k-1)\,\pi}{2N}, \\ h_k &= (\omega+\kappa) - \kappa\cos\tfrac{(k-1)\,\pi}{N}. \end{aligned} \tag{67}$$

Now we proceed to reveal the normal modes of the chain. Following (17), we calculate

$$\mathrm{Spec}(\mathsf{J}\mathbf{H}_{\mathrm{N}}) = (i\varsigma_1, ..., i\varsigma_N, -i\varsigma_1, ..., -i\varsigma_N), \tag{68}$$

with

$$\varsigma_k = \sqrt{\omega(\omega+\kappa) - \omega\kappa\cos\tfrac{(k-1)\,\pi}{N}}, \quad k = 1, ..., N. \tag{69}$$

The set (69) defines the symplectic spectrum (29) and is indeed not degenerate. The symplectic spectrum of the external oscillators is $\Lambda_{\mathrm{e}} = \Omega\mathsf{I}_4$. With these in hand, we are able to construct S_0 which is the symplectic matrix (28) that diagonalizes $\mathbf{H}_{\mathrm{e}} \oplus \mathbf{H}_{\mathrm{N}}$. By doing that, the free Hamiltonian (6) with $\mathbf{H}_{\mathrm{e}}$ and $\mathbf{H}_{\mathrm{N}}$ will be indirectly diagonalized when written in terms of the normal modes. We start by conveniently writing S_0 as

$$\mathsf{S}_0 = \mathsf{I}_4 \oplus \mathsf{S}, \tag{70}$$

being S the matrix that performs the simplectic diagonalization of $\mathbf{H}_{\mathrm{N}}$. Considering $\mathbf{M} = \mathbf{H}_{\mathrm{N}} = \mathbf{Q} \oplus \omega\,\mathsf{I}_N$ in (18), one can show that $O = \boldsymbol{O} \oplus \boldsymbol{O}$ is a solution of (19) with $\boldsymbol{O}$ defined in (67). By explicitly working with (18), it is now easy to show that $\mathsf{S} = \boldsymbol{S}\boldsymbol{O} \oplus \boldsymbol{S}^{-1}\boldsymbol{O}$ with

$$\boldsymbol{S} = \mathrm{Diag}\left(\sqrt[4]{\tfrac{\omega}{h_1}}, ..., \sqrt[4]{\tfrac{\omega}{h_N}}\right), \tag{71}$$

for h_k defined in (67). Also, it may be useful to note that

$$\mathsf{S}_{m\mu} = \sqrt{\frac{\omega}{\varsigma_m}}\,\boldsymbol{O}_{m\mu}, \quad \mathsf{S}_{m+N\mu} = 0 \quad (\mu = \alpha, \beta). \tag{72}$$

When the external oscillators are put in resonance with the m^{th} normal mode, *i.e.*, $\varsigma_m = \Omega$, the following effective Hamiltonian is obtained with application of (43) and (72)

$$\begin{aligned} \tilde{H}^{(m)}_{\mathrm{eff}} &= \frac{\hbar\epsilon\omega}{4\varsigma_m}\left(\boldsymbol{O}^2_{m\alpha} + \boldsymbol{O}^2_{m\beta}\right)\hat{a}^{\dagger}_m\hat{a}_m + \frac{\hbar\epsilon}{4}(\hat{\mathsf{a}}^{\dagger}_a\hat{\mathsf{a}}_a + \hat{\mathsf{a}}^{\dagger}_b\hat{\mathsf{a}}_b) \\ &- \frac{\hbar\epsilon\sqrt{\omega}}{4\sqrt{\varsigma_m}}\left[\boldsymbol{O}_{m\alpha}(\hat{a}_m\hat{\mathsf{a}}^{\dagger}_a + \hat{a}^{\dagger}_m\hat{\mathsf{a}}_a) + \boldsymbol{O}_{m\beta}(\hat{a}_m\hat{\mathsf{a}}^{\dagger}_b + \hat{a}^{\dagger}_m\hat{\mathsf{a}}_b)\right]. \end{aligned} \tag{73}$$

Now a few important remarks. First, one can clearly see that the resonances are not equivalent. For example, if the resonant mode is chosen to be $m = 1$, that is $\Omega = \varsigma_1$, the dynamics will be independent of the positions that the external oscillators are connected to the chain (translational invariance). In other words, there is no dependency on α and β (see Fig. 2), and this follows from $\boldsymbol{O}_{1\mu} = 1/\sqrt{N}$, $\forall\mu$, see Eq. (67). For other resonances ($\Omega = \varsigma_m$, $m \neq 1$), translational invariance is broken and the dynamics will drastically depend on α, β. For instance, if $\alpha = kN/(2m-2) + 1/2$ with $k \in \mathbb{Z}^*$, then $\boldsymbol{O}_{m\alpha} = 0$, the external oscillator a is effectively decoupled from the chain — The aforementioned positions α are nodes (zero amplitude) of high frequency modes ($m > 1$) and this results in decoupling. As a final remark, only when resonance is set with mode $m = 1$, the closed chain considered in [9] is equivalent to the open chain treated here, *i.e.*, both topologies can be described by Hamiltonian $\tilde{H}^{(1)}_{\mathrm{eff}}$

Now we turn our attention to the interaction with the environment. One can see from (70) that

$$\begin{aligned} \mathsf{S}_0\mathsf{S}_0^{\top} &= \mathsf{I}_4 \oplus \boldsymbol{S}^2 \oplus \boldsymbol{S}^{-2} \\ &= \mathsf{I}_4 \oplus \mathrm{Diag}\left(\tfrac{\omega}{\varsigma_1}, ..., \tfrac{\omega}{\varsigma_N}, \tfrac{\varsigma_1}{\omega}, ..., \tfrac{\varsigma_N}{\omega}\right), \end{aligned} \tag{74}$$

and this leads (54) to a special form whose physical interpretation is that each mode will see only a single local squeezed reservoir, as discussed in Sec.III E.

Finally, the physical situation is that of an effective dynamics comprising only the external oscillators and the m^{th} normal mode of the chain, these three subjected to local baths. Since modes other than m follow free dissipative evolutions (decoupled from a, b, and m), they do not have to be included in the description, provided our interest is in the external oscillators. Coming back to the position/momentum representation (56), we obtain

$$\tilde{H}^{(m)}_{\mathrm{eff}} = \tfrac{\epsilon}{8}\check{x}^{\dagger}\mathbf{H}_{\mathbf{q}} \oplus \mathbf{H}_{\mathbf{q}}\check{x} \tag{75}$$

with

$$\mathbf{H}_{\mathbf{q}} = \begin{pmatrix} 1 & 0 & -\mathsf{S}_{m\alpha} \\ 0 & 1 & -\mathsf{S}_{m\beta} \\ -\mathsf{S}_{m\alpha} & -\mathsf{S}_{m\beta} & (\mathsf{S}^2_{m\alpha} + \mathsf{S}^2_{m\beta}) \end{pmatrix}, \tag{76}$$

whose elements are given by (72). For (60), we have

$$\begin{aligned} \check{\mathbf{\Gamma}} &:= \mathsf{J}^{[6]}\left(\mathbf{H}_{\mathbf{q}} \oplus \mathbf{H}_{\mathbf{q}}\right) - \frac{\zeta}{2}\mathsf{I}_6, \\ \check{\mathbf{D}} &:= \hbar\zeta(\bar{n}_{\mathrm{th}} + \tfrac{1}{2})\left(\mathsf{I}_2 \oplus \tfrac{\varsigma_m}{\omega} \oplus \mathsf{I}_2 \oplus \tfrac{\omega}{\varsigma_m}\right), \end{aligned} \tag{77}$$

which, in association with the symplectic evolution (62),

$$\mathsf{E}(t) = \exp\left[\mathsf{J}(\mathbf{H}_{\mathbf{q}} \oplus \mathbf{H}_{\mathbf{q}})\,t\right] \in \mathrm{Sp}(6, \mathbb{R}) \cap \mathrm{O}(6), \tag{78}$$

allows one to obtain the time evolved CM according to the solution (61). Detailed expressions for the matrix elements constituting $\mathsf{E}(t)$ can be found in Appendix B.

V. APPLICATION: ENERGY TRANSPORT

The validity of the method developed so far is now carefully studied in a specific problem of importance for quantum technologies. This concerns the propagation of energy from a quantum system (oscillator b) to another (oscillator a) through a quantum bus (the network).

A. Non-degenerate normal modes

Let us consider the propagation of energy between the oscillators b and a through the linear chain, as depicted in Fig.2. For that, all oscillators are initially prepared in a tensor product of local vacuum states, except for b which will be considered in a thermal state (TS). Thus, the CM (10) at $t = 0$ for the global system reads

$$\mathbf{V}_0 = \mathbf{V}_{\rm T} \oplus \frac{\hbar}{2}\mathsf{I}_{2N}, \tag{79}$$

in which the CM of the subsystem (a, b) is given by

$$\mathbf{V}_{\rm T} = \frac{\hbar}{2}\begin{pmatrix} 1 & 0 \\ 0 & 2\bar{n}_b+1 \end{pmatrix} \oplus \frac{\hbar}{2}\begin{pmatrix} 1 & 0 \\ 0 & 2\bar{n}_b+1 \end{pmatrix}, \tag{80}$$

where $\bar{n}_b \geq 0$ is the average number of thermal phonons initially in the oscillator b. Notice that oscillator a is initially in the vacuum state. We will be interested in the dynamics of the average occupation number of a, and this can be extracted from the evolved CM as

$$\bar{n}_a := \langle \hat{\mathsf{a}}_a^\dagger \hat{\mathsf{a}}_a \rangle_t = \tfrac{1}{2\hbar}\left[\mathbf{V}_{11}(t) + \mathbf{V}_{33}(t)\right] - \tfrac{1}{2}. \tag{81}$$

Let us start with the ideal case of a perfectly isolated system. In this case, the evolution of $\mathbf{V}_0$ will be governed by (12) with $\boldsymbol{\Upsilon} = 0$ and $\boldsymbol{\Gamma} = \mathsf{J}\mathbf{H}$, *i.e.*,

$$\mathbf{V}(t) = \mathrm{e}^{\mathsf{J}\mathbf{H}t}\,\mathbf{V}_0\,\mathrm{e}^{-\mathbf{H}\mathsf{J}t}. \tag{82}$$

Note that $\mathrm{e}^{\mathsf{J}\mathbf{H}t} \in \mathrm{Sp}(2\mathrm{N}+4, \mathbb{R})$. Despite the apparent simplicity of this formula, it involves exponentiation of $(2N + 4) \times (2N + 4)$ matrices, a difficult task depending on the magnitude of N. However, using the method developed in Sec. III, one deals instead with exponentiation of 6×6 matrices regardless of N:

$$\check{\mathbf{V}}(t) = \mathsf{E}(t)\,\check{\mathbf{V}}_0\,\mathsf{E}^\top(t). \tag{83}$$

Of course, N can not be considered arbitrarily big. In this case, the frequency of the modes will vary in a continuum, and this spoils the RWA [9]. Now, we evaluate the average occupation number of a as

$$\check{n}_a := \tfrac{1}{2\hbar}\left[\check{\mathbf{V}}_{11}(t) + \check{\mathbf{V}}_{33}(t)\right] - \tfrac{1}{2}, \tag{84}$$

which, after using the matrix elements presented in Appendix B, become

$$\check{n}_a = 2\bar{n}_b\, F(\mathsf{S}^2_{m\alpha} + \mathsf{S}^2_{m\beta} + 1, \tfrac{\epsilon t}{4}) \tag{85}$$

with

$$F(\chi,\tau) = \frac{\mathsf{S}^2_{m\alpha}\mathsf{S}^2_{m\beta}}{\chi(\chi-1)}\left[\frac{\chi^{-1}-\cos[(\chi-1)\tau]}{(\chi-1)} + \frac{\cos(\chi\tau)}{\chi} + (1-\cos\tau)\right]. \tag{86}$$

It is interesting to notice that the energy or occupation number of oscillator a depends linearly on $\bar{n}_b$.

In Fig. 3, we compare the mean occupation number of oscillator a predicted by the exact ($\bar{n}_a$) and effective models ($\check{n}_a$). The latter involving just oscillators a, b, and normal mode $m = 1$ ($\Omega = \zeta_1 = \omega$). Additionally, we present the occupation number of oscillator b using the exact model to see how its energy is dynamically depleted to excite oscillator a. We chose a chain of moderate length ($N = 10$) in order to be able to progress computationally within the exact model.

We are working in the regime $\epsilon \ll \Omega, \varsigma_k$ ($k = 1, ..., N$), and it is clear that the simple effective model produces excellent results. Of course, as time increases, the agreement is gradually spoiled as a consequence of the fact that what supports RWA is a first-order perturbation theory which looses applicability for arbitrarily long times. This was previously observed in [9].

In order to deepen our understanding about the order of magnitude of corrections to the approximate model, we look more closely to the exact dynamics $\bar{n}_a$. Especially, the simplified model predicts that the occupation number of oscillator a vanishes for $\bar{n}_b = 0$. What does the exact model predict? To address this question, in Fig. 4 we present the time evolution of $\bar{n}_a$ for the same physical parameters used in Fig. 3, except for the initial occupation number of b, now taken to be $\bar{n}_b = 0$. What we see are high frequency and small amplitude oscillations which contribute little on average to $\bar{n}_a$. These contributions coming from small-amplitude fast oscillations are a result of terms discarded in the RWA.

As mentioned before, the effective Hamiltonian changes considerably depending on which mode is in resonance with the external oscillators. Since the dynamics of (85) is entirely determined by the function F, its analysis should reveal this dependence in a clear way. One can see, for example, that for fixed physical parameters (ϵ, $\bar{n}_b$, etc.) and resonance with mode $m = 1$, the global maximum of F, as a function of time, majorates all global maxima attained when resonance is set with other modes. Besides, only when resonance takes

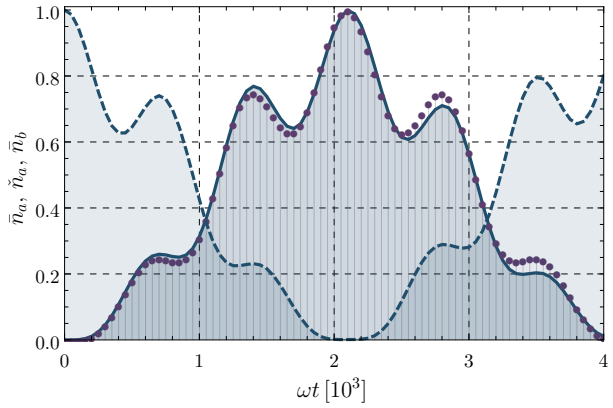


Figure 3. Mean occupation number as a function of dimensionless time ωt. Solid and dashed lines are exact evolutions for oscillators a and b, respectively, while dots refer to oscillator a using the effective model involving just a, b and normal mode $m = 1$. The chain is composed of $N = 10$ oscillators with first neighbor interaction by means o Hooke forces with $\kappa/\omega = 20$. Oscillators a and b, angular frequency $\Omega = 1$, interact with the network also through Hooke forces. They couple to network oscillators positioned at $\alpha = N$ and $\beta = 1$, respectively (ends of the chain). The coupling strength is $\epsilon/\omega = 0.03$. Oscillator b starts in a thermal state with $\bar{n}_b = 1$, while all other oscillators start in local vacuum states.

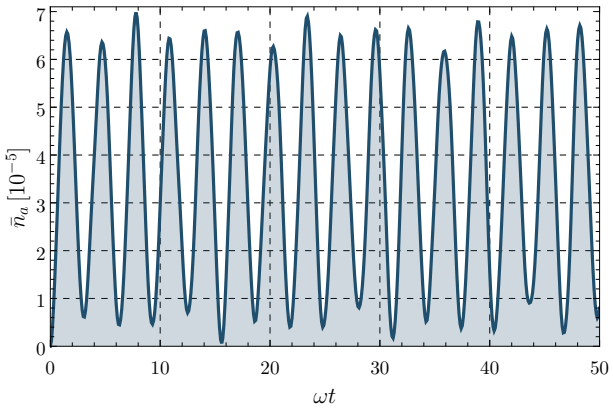


Figure 4. Exact time evolution of the mean occupation number of oscillator a for oscillator b initially prepared in a vacuum state $\bar{n}_b = 0$. The remaining parameters are kept as in Fig. 3.

place with $m = 1$, the function F is independent of α and β. This rich behavior can be explored for controlling transport in the chain [9]. In order to appreciate this dependence, we show in Fig. 5 the dynamical behavior of F for resonance with $m = 2$ and for a fixed to one of the ends of the chain. One can clearly see the dependence on β, *i.e.*, the position in the chain oscillator b is attached to.

Now, let us suppose that the energy initially in the system is not only due to oscillator b. For example, the network might as well have some initial thermal energy. Would it be possible to theoretically separate the contributions from b and network to the energy absorbed by oscillator a? To investigate this question, we still consider oscillator b initially in a thermal state with thermal occupation number $\bar{n}_b$, but now each oscillator in the network is initially found in a local thermal state, all of them at same temperature, *i.e.*, with the same thermal occupation $\bar{n}$. The CM (10) for the initial global state is then

$$\mathbf{V}_0' = \mathbf{V}_{\rm T} \oplus \tfrac{\hbar}{2}(2\bar{n}+1)\,\mathsf{I}_{2N}, \tag{87}$$

with $\mathbf{V}_{\rm T}$ as in (80). By using Eq. (84) and information in Appendix B, it is tedious but straightforward to show that

$$\check{n}_a' = \check{n}_a + 4\chi^{-2}\mathsf{S}_{m\beta}^2 \sin^2\left(\tfrac{\chi\epsilon t}{8}\right)\bar{n}, \tag{88}$$

where $\check{n}_a$ is given in (85) and χ is implicitly defined in (85) and (86). From this, some comments are in order. First of all, one can see that the mean occupation number of oscillator a is indeed the result of distinct contributions from oscillator b and network. The latter contributes with the term which does not depend on the occupation number of b, that is $4\chi^{-2}\mathsf{S}_{m\beta}^2 \sin^2\left(\frac{\chi\epsilon t}{8}\right)\bar{n}$. It is worth noticing that this contribution increases with the temperature of the network oscillators as one could expect. The separation between contributions coming from b and normal mode m is possible because the effective model involves only three bodies and no direct coupling between a and b. Being able to extract this kind of information from a complex system is one of the main advantages of simplified but accurate models. Another comment concerns the relatively small flux of energy from the network to oscillator a. Let us consider again the chain with $N = 10$ oscillators used to produce Fig. 3. Although there were initially a total number of ten thermal phonons in the network (one for each of the ten oscillators), only 2.8% of them is absorbed by a. This can be seen from Fig. 6 where we show the time evolution of (88) considering oscillator b in the vacuum state, while the ten oscillators of the network are prepared in local thermal states with $\bar{n} = 1$. The physical explanation for this observation relies on the fact that the initial ten thermal photons are shared by all normal modes. When resonance is set to one of these modes, the energy in the other modes becomes unavailable to a or b.

We now move to a scenario where the oscillators (external and network) are subjected to local thermal baths whose action on system is due to (49). Now, the equation of motion for the CM is given by (12) with

$$\mathbf{\Gamma} = -\frac{\zeta}{2}\mathsf{I}_{2N+4} + \mathbf{J}\mathbf{H}, \;\; \mathbf{D} = \hbar\zeta(\bar{n}_{\rm th} + \tfrac{1}{2})\mathsf{I}_{2N+4}, \tag{89}$$

and its formal solution is given by (14). It is clear that the exponentiation of $(2N+4)\times(2N+4)$ causes computational

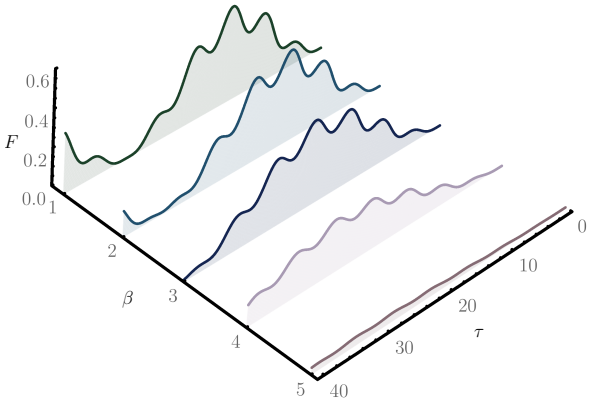


Figure 5. Dependence of function F defined in (86) on β and scaled time $\tau = \epsilon t/4$. We consider $\alpha = N = 10$ and $m = 2$. The remaining parameters are kept as in Fig. 3.

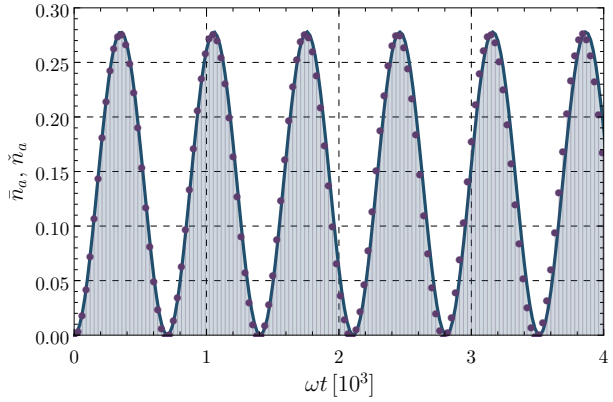


Figure 6. Mean occupation number as a function of dimensionless time ωt. The physical parameters are that of Fig. 3, except for the initial state of network oscillators which now is the product of local thermal states with $\bar{n} = 1$, and the initial state of b which now is vacuum, *i.e.*, $\bar{n}_b = 0$.

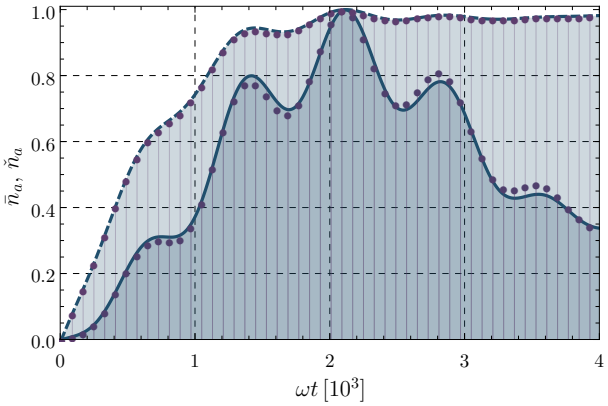


Figure 7. Mean occupation number as a function of dimensionless time ωt. Each of the $N+2$ oscillators are attached to thermal reservoirs with $\bar{n}_{\rm th} = 1$. Two values of ζ are considered: $\zeta = 0.01$ (dashed line) and $\zeta = 0.001$ (solid line). Dots are obtained using the effective model involving just a, b and normal mode $m = 1$. The initial state and the remaining parameters are kept the same as in Fig. 3.

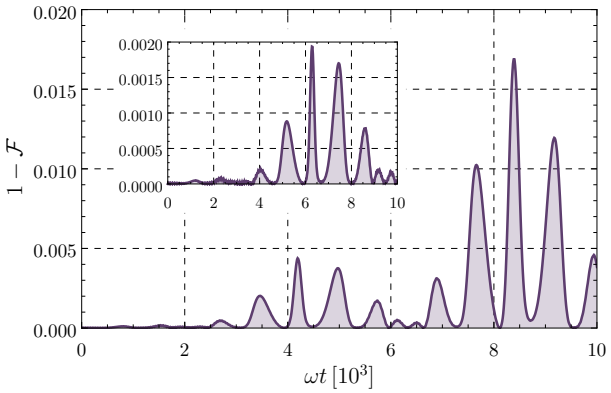


Figure 8. Dynamics of $1-\mathcal{F}$, where $\mathcal{F}$ is the fidelity between evolved density operators for oscillator a using the exact and effective models. The physical parameters in the main plot are the same as in Fig. 3, but in the inset the coupling constant with the network is slightly reduced to $\epsilon/\omega = 0.01$.

difficulties already for moderately high N. Besides, it is basically impossible to progress analytically within this many body description. Using the results developed here, one can give a clear and accurate description of the dynamics of the external oscillators working with (61) and (77) instead. Now, the matrices to be exponentiated are just 6×6, and one may show that

$$\check{\mathbf{V}}(t) = \mathrm{e}^{-\zeta t}\mathsf{E}(t)\,\check{\mathbf{V}}_0\,\mathsf{E}^{\top}(t) + \frac{1}{\zeta}\left(1-\mathrm{e}^{-\zeta t}\right)\check{\mathbf{D}}, \tag{90}$$

with $\mathsf{E}(t)$ still given by (78). It is interesting to notice that the unitary part of this evolution, already present in (83), is now exponentially attenuated with characteristic time ζ^{-1} in the above equation.

Let us now then compare the predictions using the approximate effective model developed here and the exact dynamics. In Fig. 7, we present the mean occupation number for oscillator a following both descriptions. We keep notation used in the closed system case. Giving the general agreement between both descriptions, it is clear that our methodology works well also for the open system case. This plot shows that the higher the relaxation constant ζ, the sooner the occupation number of oscillator a reaches that of the thermal reservoir it is interacting with, which is $\bar{n}_{\rm th} = 1$. As time passes, the presence of the initial state $\mathbf{V}_0$ in (90) is progressively erased by $\mathrm{e}^{-\zeta t}$, which makes the CM tend to

$$\lim_{t\to\infty}\check{\mathbf{V}}(t) = \frac{1}{\zeta}\check{\mathbf{D}}, \tag{91}$$

showing that not only a thermalizes with its local bath, but also b and mode m do the same.

The plot in Fig. 7 presents another interesting feature. The effective model is based on the RWA, whose validity is justified with first-order perturbation theory. Then, the validity of the approximation is limited for finite times. However, we see that the simplified model gives the correct asymptotic limit, as seen clearly in the case $\zeta = 0.01$. It can be seen with $\zeta = 0.001$ as well but at longer times (not shown in the plot). The reason why the long time regime is not spoiled is that RWA is made only for the Hamiltonian part of the dynamics, which becomes less and less important with time, see (90) and (91). The agreement between the complete exact model and our simplified model also shows that the decoupling mechanism in terms of local reservoirs in the modes works perfectly well. In summary, our model gives very accurate results for the initial cycles of the dynamics and for the long time limit when each oscillator is coupled to a thermal bath in the conditions discussed here. If the system is isolated, *i.e.*, no local reservoirs are attached to the oscillators, the accuracy will just slowly and gradually be spoiled with time as seen before.

Now, we want to be more quantitative in terms of the accuracy of the simplified model developed here. In order to do that, we will investigate the density matrix for oscillator a predicted by exact and approximate models, denoted by $\hat{\rho}_a$ and $\check{\rho}_a$, respectively. We will employ the fidelity $\mathcal{F}$ between these states as a figure of merit [24]:

$$\mathcal{F} := \left[\mathrm{Tr}\left(\sqrt{\hat{\rho}_a}\check{\rho}_a\sqrt{\hat{\rho}_a}\right)^{\frac{1}{2}}\right]^2 \leq 1. \tag{92}$$

Since we are working with Gaussian states centered at origin of the phase space, one can show that the above formula reduces to [24]

$$\mathcal{F} = \frac{2}{\sqrt{\det(\mathbf{V_a}+\check{\mathbf{V}}_\mathbf{a})+\det(\mathbf{V_a}-1)(\check{\mathbf{V}}_\mathbf{a}-1)}-\sqrt{\det(\mathbf{V_a}-1)(\check{\mathbf{V}}_\mathbf{a}-1)}}, \tag{93}$$

where $\mathbf{V_a}$ and $\check{\mathbf{V}}_\mathbf{a}$ are, respectively, the CMs of subsystem a obtained with (82) and (83)

$$\mathbf{V_a} = \begin{pmatrix}\mathbf{V}_{11} & \mathbf{V}_{13}\\ \mathbf{V}_{31} & \mathbf{V}_{33}\end{pmatrix}, \quad \check{\mathbf{V}}_\mathbf{a} = \begin{pmatrix}\check{\mathbf{V}}_{11} & \check{\mathbf{V}}_{13}\\ \check{\mathbf{V}}_{31} & \check{\mathbf{V}}_{33}\end{pmatrix}. \tag{94}$$

In Fig. 8, we plot $(1-\mathcal{F})$ as a function of time for the same physical parameters considered in Fig. 3. Just like in the plots of occupation number, here too the fidelity progressively

deteriorates in time, which corresponds to the breaking of the RWA for the closed system. However, many oscillations are necessary to this deterioration to cause appreciable deviations. It is interesting to see that just a slightly reduction of ϵ (inset of Fig. 8) is enough to make the deterioration even weaker. This is in complete agreement with the first-order time perturbation theory justification of RWA used in this paper.

B. Degenerate normal modes

To emphasize the generality of effective descriptions based on the methodology developed here, let us now consider the system depicted in Fig. 9. It opens up the possibility for studying the resonance between the external oscillators and degenerate normal modes.

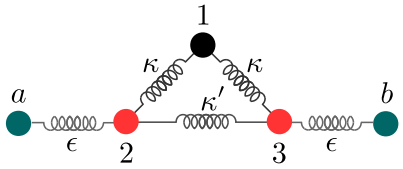


Figure 9. Triangular network of oscillators, where ϵ, κ and κ' are coupling constants for oscillators coupled by springs (Hooke's forces).

The free Hamiltonian of the network is written as in Eq. (6) but now with

$$\mathbf{H}_{\rm N} = \mathbf{Q} \oplus \omega\, \mathsf{I}_3, \tag{95}$$

where the 3×3 potential matrix is given by

$$\mathbf{Q} = \begin{pmatrix} \kappa+\omega & -\frac{1}{2}\kappa & -\frac{1}{2}\kappa \\ -\frac{1}{2}\kappa & \frac{1}{2}(\kappa+\kappa')+\omega & -\frac{1}{2}\kappa' \\ -\frac{1}{2}\kappa & -\frac{1}{2}\kappa' & \frac{1}{2}(\kappa+\kappa')+\omega \end{pmatrix}. \tag{96}$$

The symplectic spectrum (16) reads now

$$\begin{aligned} &\varsigma_1 = \omega, \;\; \varsigma_2 = \sqrt{\omega(\omega+\kappa/2+\kappa')}, \\ &\varsigma_3 = \sqrt{\omega(\omega+3\kappa/2)}. \end{aligned} \tag{97}$$

From (19), one can calculate the matrix that performs the symplectic diagonalization of the free Hamiltonian. The same structure as in (70) is found here too, *i.e.*, $\mathsf{S} = \boldsymbol{S}\boldsymbol{O}\oplus\boldsymbol{S}^{-1}\boldsymbol{O}$, but now with

$$\boldsymbol{S} = \mathrm{Diag}\left(\sqrt[4]{\tfrac{\omega}{\varsigma_1}}, \sqrt[4]{\tfrac{\omega}{\varsigma_2}}, \sqrt[4]{\tfrac{\omega}{\varsigma_3}}\right), \boldsymbol{O} = \begin{pmatrix} \frac{1}{\sqrt{3}} & \frac{1}{\sqrt{3}} & \frac{1}{\sqrt{3}} \\ 0 & -\frac{1}{\sqrt{2}} & \frac{1}{\sqrt{2}} \\ -\frac{\sqrt{2}}{\sqrt{3}} & \frac{1}{\sqrt{6}} & \frac{1}{\sqrt{6}} \end{pmatrix}, \tag{98}$$

being $\boldsymbol{O}$ the orthogonal matrix that performs the Euclidean diagonalization of the potential matrix $\mathbf{Q}$.

Considering $\kappa' \neq \kappa$, the effective Hamiltonian is the same as in (75) with $\mathbf{H}_{\mathbf{q}}$ (76) defined in terms of $\mathsf{S}_{m\mu}$ calculated using S (98) with index $m = 1,2,3$ and $\mu = 2,3$. The matrices in (77) are also the same, provided we update the symplectic eigenvalues to (97). With this replacement, results (85), (88), (90), and (91) stay valid.

On the other hand, if $\kappa = \kappa'$, the symplectic spectrum is degenerate since $\varsigma_2 = \varsigma_3$. As prescribed in Sec. III D, if the external oscillators are set in resonance with this degenerate mode, $\Omega = \varsigma_2 = \varsigma_3$, operator (63) becomes $\check{x} = (\hat{\mathsf{q}}_a, \hat{\mathsf{q}}_b, \hat{q}_2, \hat{q}_3, \hat{\mathsf{p}}_a, \hat{\mathsf{p}}_b, \hat{p}_2, \hat{p}_3)^{\dagger}$, and the effective dynamics will be governed by (46) which, for the present case reads $\hat{H}^{(2,3)}_{\rm eff} = \frac{\epsilon}{8}\check{x}^{\dagger}\mathbf{H}_{\mathbf{q}} \oplus \mathbf{H}_{\mathbf{q}}\check{x}$ with

$$\mathbf{H}_{\mathbf{q}} = \begin{pmatrix} 1 & 0 & -\mathsf{S}_{22} & -\mathsf{S}_{32} \\ 0 & 1 & -\mathsf{S}_{23} & -\mathsf{S}_{33} \\ -\mathsf{S}_{22} & -\mathsf{S}_{23} & \mathsf{S}_{22}^2+\mathsf{S}_{23}^2 & \mathsf{S}_{22}\mathsf{S}_{32}+\mathsf{S}_{23}\mathsf{S}_{33} \\ -\mathsf{S}_{32} & -\mathsf{S}_{33} & \mathsf{S}_{22}\mathsf{S}_{32}+\mathsf{S}_{23}\mathsf{S}_{33} & \mathsf{S}_{32}^2+\mathsf{S}_{33}^2 \end{pmatrix}, \tag{99}$$

to be evaluated with (98). Now one can calculate $\mathsf{E}(t) = \exp\left[\mathsf{J}\mathbf{H}_{\rm eff}\, t\right] \in \mathrm{Sp}(8,\mathbb{R})$ and determine the dynamics of the occupation number for oscillator a which is plotted in Fig. 10.

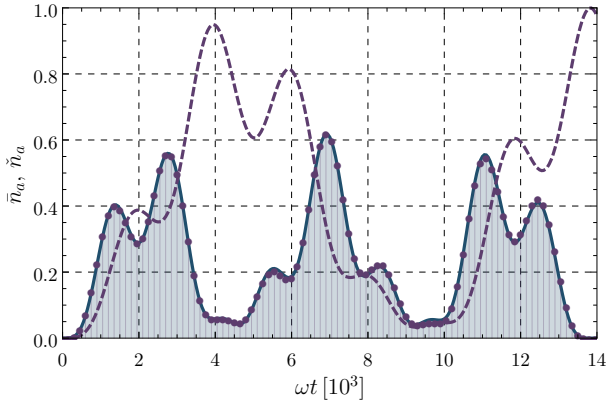


Figure 10. Mean occupation number as a function of dimensionless time ωt. The topology depicted Fig. 9 is used with $\kappa = \kappa'$, and resonance is taken with the resulting degenerate modes $\Omega = \varsigma_2 = \varsigma_3$. As before, the solid line is exact and dots refer to the approximate model. The dashed line corresponds to the dynamics where one mistakably and naively includes only mode 3 in the effective model. We consider $\kappa/\omega = \kappa'/\omega = 1/3$ and $\epsilon/\omega = 1/600$. The initial state of oscillator b is thermal with $\bar{n}_b = 1$, and the other oscillators are in local vacuum states.

Again, it is remarkable the agreement of the simplified model (now two-mode) with exact dynamics. For comparison, it is also shown the behavior with just one mode in the effective description. The reason it to draw our attention to the fact that degeneracy should be taken into account carefully through the effective description (46). For longer times, not shown in the plot, the mean occupation number $\bar{n}_a$ attain $\bar{n}_b = 1$ within the precision of the numerical treatment of the original model. The effective model can not be used at such long times as previously discussed.

The inclusion of thermal baths to each oscillator is made along the lines of the previous examples (77). Now, one should only be careful to take into account the presence of

one more mode, *i.e.*,

$$\begin{aligned}\check{\mathbf{\Gamma}} &:= \mathsf{J}^{[8]}\left(\mathbf{H_q}\oplus\mathbf{H_q}\right)-\frac{\zeta}{2}\mathsf{I}_8,\\ \check{\mathbf{D}} &:= \hbar\zeta(\bar{n}_{\rm th}+\tfrac{1}{2})\left(\mathsf{I}_2\oplus\tfrac{\varsigma_2}{\omega}\oplus\tfrac{\varsigma_3}{\omega}\oplus\mathsf{I}_2\oplus\tfrac{\omega}{\varsigma_2}\oplus\tfrac{\omega}{\varsigma_3}\right).\end{aligned} \tag{100}$$

The effect is essentially the same as in Fig. 7 and, for this reason, we will not add a plot for this case.

Control of errors due to the approximations made to obtain (99) is again made through inspection of $(1-\mathcal{F})$, with $\mathcal{F}$ defined in (93). This is presented in Fig. 11. One can see that, in agreement to what is shown in Fig. 10, fidelility is quite high meaning that the effective model produces accurate results even in the case of degeneracy. As expected, the fidelity slowly degrades with time.

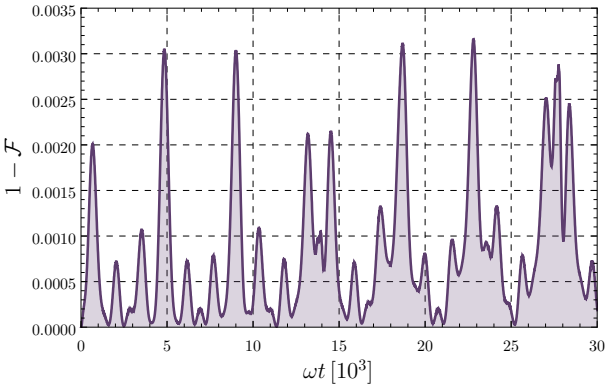


Figure 11. Dynamics of $1-\mathcal{F}$, where $\mathcal{F}$ is the fidelity between evolved density operators for oscillator a using the exact and effective models. This is a case with degeneracy and the parameters are those considered in Fig. 10.

C. Beyond the Hooke's Law

In previous examples, the interaction between oscillators in the network follows Hooke's law, *i.e.*, spring-like couplings. This implies that the effective Hamiltonian in (56) does not present crossed terms involving position and momentum. Mathematically, this is the same as $\mathbf{C_{qp}}$ null in (58). Since the method is applicable to any positive definite Hamiltonian, this section advances to the consideration of a toy model where momentum and position cross in the interaction Hamiltonian. For this purpose, we consider now that (6) is defined with

$$\mathbf{H}_{\rm N}=\begin{pmatrix}\omega\mathsf{I}_3 & \mathbf{C}\\ \mathbf{C} & \omega\mathsf{I}_3\end{pmatrix},\quad \mathbf{H}_{\rm e}=\Omega\mathsf{I}_4, \tag{101}$$

where we considered $N=3$ oscillators in the network and

$$\mathbf{C}=\frac{\gamma}{2}\mathsf{I}_3-\frac{1}{\sqrt{2}}\begin{pmatrix}0&\kappa&0\\ \kappa&0&\kappa\\ 0&\kappa&0\end{pmatrix}. \tag{102}$$

The above matrix will lead to $-\frac{\kappa}{\sqrt{2}}(\hat{q}_1\hat{p}_2+\hat{q}_2\hat{p}_1+\hat{q}_3\hat{p}_2+\hat{q}_2\hat{p}_3)+\gamma\sum_{j=1}^{3}(\hat{q}_i\hat{p}_i+\hat{p}_i\hat{q}_i)$ in the network Hamiltonian.

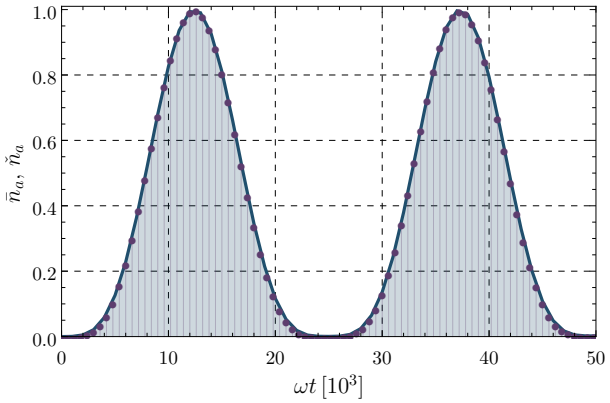


Figure 12. Mean occupation number of oscillator a as a function of dimensionless time ωt. The Hamiltonian of the network is given by (101) with $\kappa/\omega=0.5$ and $\gamma/\omega=0.2$. The solid line is the exact time evolution, while the dots are the result of the effective model. Oscillators a and b possess frequency $\Omega=\varsigma_1$ and are coupled, respectively, to oscillators $\alpha=1$ and $\beta=3$ in the network with $\epsilon/\omega=0.001$. Oscillator b is initially in a thermal state with $\bar{n}_b=1$ and all other oscillators are initially in local vacuum states.

Since $\mathbf{H}_{\rm N}$ must be positive definite, condition $\omega>\kappa+\gamma$ has to be imposed. The external oscillators, a and b, interact with the network as usual, see (7).

For this example, symplectic diagonalization of $\mathbf{H}_{\rm N}$ results in

$$\begin{aligned}&\varsigma_1=\sqrt{\omega^2-(\kappa+\gamma)^2},\ \ \varsigma_2=\sqrt{\omega^2-(\kappa-\gamma)^2},\\ &\varsigma_3=\sqrt{\omega^2-\gamma^2},\end{aligned} \tag{103}$$

from which one obtains the matrix that performs the symplectic diagonalization of $\mathbf{H}_{\rm N}$. This is now written as $\mathsf{S}_{\rm N}=(\boldsymbol{S}\oplus\boldsymbol{S}^{-1})\mathsf{R}(\boldsymbol{O}\oplus\boldsymbol{O})$, where

$$\begin{aligned}\boldsymbol{S}&=\mathrm{Diag}\left(\sqrt[4]{\tfrac{\omega-\kappa-\gamma}{\omega+\kappa+\gamma}},\sqrt[4]{\tfrac{\omega+\kappa-\gamma}{\omega-\kappa+\gamma}},\sqrt[4]{\tfrac{\omega-\gamma}{\omega+\gamma}}\right),\\ \mathsf{R}&=\frac{1}{\sqrt{2}}\begin{pmatrix}\mathsf{I}_3&\mathsf{I}_3\\ -\mathsf{I}_3&\mathsf{I}_3\end{pmatrix},\\ \boldsymbol{O}&=\begin{pmatrix}\frac{1}{2}&-\frac{1}{\sqrt{2}}&\frac{1}{2}\\ \frac{1}{2}&\frac{1}{\sqrt{2}}&\frac{1}{2}\\ -\frac{1}{\sqrt{2}}&0&\frac{1}{\sqrt{2}}\end{pmatrix},\end{aligned} \tag{104}$$

being $\boldsymbol{O}$ the orthogonal matrix that performs Euclidean diagonalization of $\mathbf{C}$. Writing the effective Hamiltonian (56) for $\Omega=\varsigma_1$, we can work on the time evolution of the covariance matrix (82) to obtain the mean occupation number of the oscillator a, as plotted in Fig. 12. Again, the effective model agrees quite well with the exact dynamics. The inclusion of local thermal baths would follow just like before, since again $\mathsf{S}_{\rm N}\mathsf{S}_{\rm N}^{\top}$ is a diagonal matrix.

Fidelity is again used to infer the quality of the approximations made to obtain the simplified model, see Fig. 13. The result shows that the accuracy of the effective description is again remarkable.

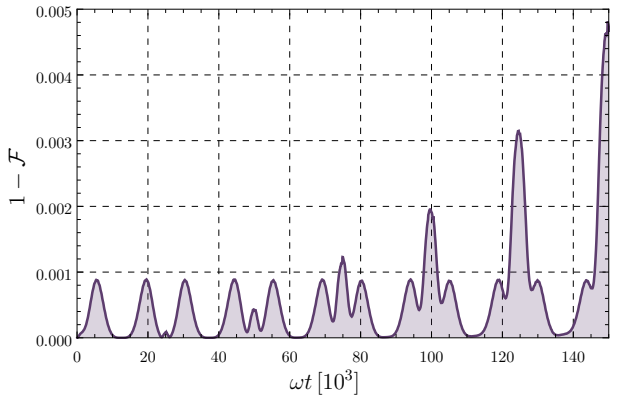


Figure 13. Dynamics of $1-\mathcal{F}$, where $\mathcal{F}$ is the fidelity between evolved density operators for oscillator a using the exact and effective models. This plot refers to the case considered in Fig. 12.

VI. FINAL REMARKS

We have described a general method to obtain useful and accurate effective descriptions of large open systems formed by coupled harmonic oscillators. The idea is that two external oscillators weakly coupled to a network of harmonic oscillators may have their dynamics effectively described by a model with just a few coupled degrees of freedom. This was first seen for the linear case of first neighbor coupled oscillators with no degeneracy nor thermal reservoirs in [9]. We improve and expand this idea by considering any topology of the network and by including environments for all elements of the system. For the unitary case, the only restriction is that the system Hamiltonian must be positive definite. When environments are attached to the oscillators, we show that further structural restrictions must be imposed to grant the simplified descriptions. In general, we showed that the number of effectively coupled constituents depends on the nature of the symplectic spectrum of the Hessian of the Hamiltonian and resonances.

As an application and illustration of the method, we consider the problem of propagation of energy through the network. Meaningful and informative analytical results could be obtained in the scope of the simplified model. We also presented how fidelity between the evolved states under exact and effective descriptions behaves, and the result shows that the accuracy of the simplified model is quite remarkable. Different topologies are used to illustrate the applicability of the methodology presented here.

It is worthwhile noticing that instead of coupling single harmonic oscillators to the network, one could have networks coupled to networks and obtain simplified models involving few coupled normal modes of different networks. In this case, the first step is symplectic diagonalization of each network and then, through resonances, end up with an effective model following our recipe.

Our work considers finite networks as environments for the two external oscillators in contrast to the typical baths necessary to model a system-reservoir interaction. In the latter, the network is formed by an infinity set of harmonic oscillators or continuum spectrum of modes. Our approach is of interest because it applies to this intermediate case where the network is big enough for not being amenable to analytical exact treatment and, at the same time, it is not big enough for allowing the usual approximations that follow from interaction with a bath. These approximations are needed, in general, for ending up with a useful master equation.

It is our opinion that the present study can contribute to studies involving transport of different physical resources in coupled harmonic systems by allowing effective descriptions amenable to analytical progress. This is important to the evaluation, for example, of limits in channel capacities or even stationary heat currents, just to name a few direct applications.

During the the revision of this work, we became aware of [26] which treats a similar system but from a different point of view whose approach is subjected to different limits of validity and aims than ours.

ACKNOWLEDGMENTS

FN and FLS are supported by the CNPq "Ciência sem Fronteiras" programme through the "Pesquisador Visitante Especial" initiative (grant nr. 401265/2012-9). FLS is a member of the Brazilian National Institute of Science and Technology of Quantum Information (INCT-IQ) and acknowledges partial support from CNPq (grant nr. 307774/2014-7).

APPENDIX

Appendix A: Rotating Wave Approximation

Consider two interacting harmonic oscillators (frequencies ω_1 and ω_2) whose dynamics is ruled by Hamiltonian $\hat{H} = \hat{H}_0 + \hat{H}_I$, where

$$\begin{aligned}\hat{H}_0 &= \hbar\omega_1\hat{a}_1^\dagger\hat{a}_1 + \hbar\omega_2\hat{a}_2^\dagger\hat{a}_2,\\ \hat{H}_I &= \hbar\sum_{j\neq k}\eta_{jk}\hat{a}_j^\dagger\hat{a}_k + \hbar\sum_{j,k}\xi_{jk}\hat{a}_j\hat{a}_k + \xi_{jk}^*\hat{a}_j^\dagger\hat{a}_k^\dagger,\end{aligned} \tag{A-1}$$

η_{jk} and ξ_{jk} time independent arbitrary numbers, $\hat{a}_j$ is the annihilation operator of the oscillator j and $i,j=1,2$. With respect to $\hat{H}_0$, the interaction picture Hamiltonian reads

$$\tilde{H}_I = \hbar\sum_{j\neq k}\eta_{jk}\tilde{a}_j^\dagger\tilde{a}_k + \hbar\sum_{j,k}\xi_{jk}\tilde{a}_j\tilde{a}_k + \xi_{jk}^*\tilde{a}_j^\dagger\tilde{a}_k^\dagger, \tag{A-2}$$

where $\tilde{a}_j = \mathrm{e}^{-i\omega_j t}\hat{a}_j$ and $\hat{a}_j$. Since the free Hamiltonian $\hat{H}_0$ is that of non-interacting oscillators, its eigenvectors are just the tensor product of Fock states *i.e.*, $|\Psi\rangle = |\mathfrak{n}_1,\mathfrak{n}_2\rangle$, where $\{|\mathfrak{n}_j\rangle; j=1,2\}$ are the eigenstates of $\hat{a}_j^\dagger\hat{a}_j$.

Treating $\hat{H}_I$ as a perturbation to $\hat{H}_0$, first order time dependent perturbation theory reveals that the transition probability between two eigenstates of $\hat{H}_0$, denoted $|\Psi\rangle$ and $|\Psi'\rangle$, is given

by [22]

$$\mathcal{P}_{\Psi\mapsto\Psi'} = \frac{1}{\hbar^2}\left|\int_0^\tau {}_I\langle\Psi|\tilde{H}_I|\Psi'\rangle_I\, dt\right|^2, \tag{A-3}$$

where $|.\rangle_I$ denotes a ket in the interaction picture. In general, $\hat{H}_I$ can be seen as a perturbation to $\hat{H}_0$ provided

$$\Delta(\Psi') := |\langle\Psi|\tilde{H}_I|\Psi'\rangle|\,|\delta_{\Psi'}|^{-1} \ll 1, \tag{A-4}$$

where

$$\delta_{\Psi'} := \langle\Psi|\hat{H}_0|\Psi\rangle - \langle\Psi'|\hat{H}_0|\Psi'\rangle. \tag{A-5}$$

For (A-2), it is easy to show that

$$\mathcal{P}_{\Psi\mapsto\Psi'} = 2|\Delta(\Psi')|^2[1-\cos(\tfrac{1}{\hbar}\delta_{\Psi'}\tau)]. \tag{A-6}$$

The non-null terms in $\langle\Psi|\tilde{H}_I|\Psi'\rangle$ will give rise to finite transition probabilities that can be divided in two classes: energy conserving and non-energy conserving. Energy conserving transitions are those in which a quantum of energy is simultaneously created in one oscillator and destroyed in the other. In the interaction Hamiltonian (A-2), terms responsible for these transitions are those proportional to $\tilde{a}_j^\dagger\tilde{a}_k$ for $i\neq j$. On the other hand, terms like $\hat{a}_j\hat{a}_k$ and $\hat{a}_j^\dagger\hat{a}_k^\dagger$ cause the net destruction or creation of two quanta of energy, either in one mode or one quantum in each mode. For the energy conserving transitions, Eq. (A-4) results in

$$\Delta(\Psi'_{\rm c}) = \left|\frac{\eta_{jk}\,\langle\mathfrak{n}_1,\mathfrak{n}_2|\hat{a}_j^\dagger\hat{a}_k|\Psi'_{\rm c}\rangle}{\omega_j-\omega_k}\right|, \tag{A-7}$$

while for non-energy conserving ones it results in

$$\Delta(\Psi'_{\rm nc}) = \left|\frac{\xi_{jk}\,\langle\mathfrak{n}_1,\mathfrak{n}_2|\hat{a}_j\hat{a}_k|\Psi'_{\rm nc}\rangle}{\omega_j+\omega_k}\right|, \tag{A-8}$$

or

$$\Delta(\Psi'_{\rm nc}) = \left|\frac{\xi^*_{jk}\,\langle\mathfrak{n}_1,\mathfrak{n}_2|\hat{a}_j^\dagger\hat{a}_k^\dagger|\Psi'_{\rm nc}\rangle}{\omega_j+\omega_k}\right|. \tag{A-9}$$

Now, it is worth noticing that if one approaches exact resonance ($\omega_j=\omega_k$), energy conserving transitions (A-7) will turn (A-6) into

$$\mathcal{P}_{\Psi\mapsto\Psi'_{\rm c}} \propto \frac{\tau^2}{\hbar^2}, \tag{A-10}$$

representing a quadratically growth, while the non-conserving energy transitions (A-8) and (A-9) will still produce limited oscillations (A-6) with very small amplitudes that are proportional to $1/(\omega_1+\omega_2)$. Consequently, the importance of the energy conservative terms soon supplants the importance of the non-conserving ones. Even in the case where one does not have exact resonance, the relative importance of the two kind of transitions will still favor the energy conserving ones, provided $|\omega_1-\omega_2|\ll|\omega_1+\omega_2|$. This is a much more relaxed condition compared to exact resonance. To see this, let us consider the common scenario where η_{jk} and ξ_{jk} have the same order of magnitudes. Then, from (A-6), (A-7), (A-8), and (A-9), it is easy to check that, apart from the limited oscillating functions, the relative importance of amplitudes is

$$\frac{\mathcal{P}_{\Psi\mapsto\Psi'_{\rm c}}}{\mathcal{P}_{\Psi\mapsto\Psi'_{\rm nc}}} \approx \frac{|\omega_1+\omega_2|}{|\omega_1-\omega_2|}. \tag{A-11}$$

Based on these considerations, one can drop terms in the interaction picture Hamiltonian which oscillate with the sum of frequencies compared to the ones oscillating with the difference of frequencies. Alternatively, one can say that energy conserving transitions are the only ones to be kept in the Hamiltonian. This elimination of rapidly oscillating terms in the Hamiltonian is called RWA, regardless of whether one has exact or approximate resonance in the sense $|\omega_1-\omega_2|\ll|\omega_1+\omega_2|$.

A word of caution is in order here. The RWA demands that the interaction part of the Hamiltonian $\hat{H}_I$, where the terms to be neglected lie, should be weak compared to the free part $\hat{H}_0$. For (A-1), this is guaranteed when $\eta_{jk},\xi_{jk}\ll\omega_1,\omega_2$. In this case, we were able to justify the RWA through first order perturbation theory. Otherwise, there is no reason for RWA to be valid. At higher orders, energy conserving and non-energy conserving terms mix in the perturbative series due to powers of $\hat{H}_I$.

Finally, in the RWA, and back to the Schrödinger picture, the system Hamiltonian will be

$$\hat{H}_{\rm eff} = \hbar(\omega_1\hat{a}_1^\dagger\hat{a}_1+\omega_2\hat{a}_2^\dagger\hat{a}_2+\eta_{12}\hat{a}_1^\dagger\hat{a}_2+\eta_{12}^*\hat{a}_2^\dagger\hat{a}_1). \tag{A-12}$$

Appendix B: Matrix $\mathsf{E}(t)$ and Auxiliary Functions

The simplectic matrix in (78) is written as

$$\mathsf{E}(t) = \begin{pmatrix}\mathbf{C} & \mathbf{S}\\ -\mathbf{S} & \mathbf{C}\end{pmatrix}, \tag{B-1}$$

where we defined the matrices $\mathbf{C}=\cos(\mathbf{H_q}t)$ and $\mathbf{S}=\sin(\mathbf{H_q}t)$ with $\mathbf{H_q}$ given by Eq. (76). Explicitly,

$$\begin{aligned}
\mathbf{C}_{11} &= \chi^{-1}[1+(\chi-1)\cos(\chi\tau)],\\
\mathbf{C}_{12} &= \mathbf{C}_{21} = \tfrac{2\mathsf{S}_{m\alpha}}{\chi}\sin^2\left(\tfrac{\chi\tau}{2}\right),\\
\mathbf{C}_{13} &= \mathbf{C}_{31} = \tfrac{2\mathsf{S}_{m\beta}}{\chi}\sin^2\left(\tfrac{\chi\tau}{2}\right),\\
\mathbf{C}_{22} &= \tfrac{\mathsf{S}^2_{m\beta}}{(\chi-1)}\cos\tau + \tfrac{\mathsf{S}^2_{m\alpha}}{\chi(\chi-1)}[(\chi-1)+\cos(\chi\tau)],\\
\mathbf{C}_{23} &= \mathbf{C}_{32} = \tfrac{\mathsf{S}_{m\alpha}\mathsf{S}_{m\beta}}{\chi(\chi-1)}[(\chi-1)-\chi\cos\tau+\cos(\chi\tau)],\\
\mathbf{C}_{33} &= \tfrac{\mathsf{S}^2_{m\alpha}}{(\chi-1)}\cos\tau + \tfrac{\mathsf{S}^2_{m\beta}}{\chi(\chi-1)}[(\chi-1)+\cos(\chi\tau)],
\end{aligned}$$

and

with $\tau := \epsilon t/4$, and $\chi := \mathsf{S}_{m\alpha}^2 + \mathsf{S}_{m\beta}^2 + 1$.

$$
\begin{aligned}
\mathbf{S}_{11} &= \tfrac{\chi-1}{\chi}\sin(\chi\tau),\\
\mathbf{S}_{12} = \mathbf{S}_{21} &= -\tfrac{\mathsf{S}_{m\alpha}}{\chi}\sin(\chi\tau),\\
\mathbf{S}_{13} = \mathbf{S}_{31} &= -\tfrac{\mathsf{S}_{m\beta}}{\chi}\sin(\chi\tau),\\
\mathbf{S}_{22} &= \tfrac{\mathsf{S}_{m\alpha}^2}{(\chi-1)\chi}\sin(\chi\tau) + \tfrac{\mathsf{S}_{m}^2}{(\chi-1)}\sin\tau,\\
\mathbf{S}_{23} = \mathbf{S}_{32} &= \tfrac{\mathsf{S}_{m\beta}\mathsf{S}_{m\alpha}}{\chi(\chi-1)}[\sin(\chi\tau) - \chi\sin\tau],\\
\mathbf{S}_{33} &= \tfrac{\mathsf{S}_{m\beta}^2}{\chi(\chi-1)}\sin(\chi\tau) + \tfrac{\mathsf{S}_{m\alpha}^2}{(\chi-1)}\sin\tau, \qquad \text{(B-2)}
\end{aligned}
$$

[1] E. Buks & M.L. Roukes, *Electrically tunable collective response in a coupled micromechanical array*, J. Microelectromech. Syst. *11*, 802 (2002).

[2] J. Eisert, M.B. Plenio, S. Bose & J. Hartley, *Towards Quantum Entanglement in Nanoelectromechanical Devices*, Phys. Rev. Lett. **93**, 190402 (2004), arXiv:quant-ph/0311113.

[3] A. Bermudez, T. Schaetz & D. Porras, *Synthetic Gauge Fields for Vibrational Excitations of Trapped Ions*, Phys. Rev. Lett **107**,150501 (2011), arXiv:1104.4734 [quant-ph].

[4] Q. Lin et al, *Coherent mixing of mechanical excitations in nano-optomechanical structures*, Nature Photonics **4**, 236 (2010), arXiv:0908.1128 [physics.optics].

[5] F. Massel et al, *Multimode circuit optomechanics near the quantum limit*, Nature Communications **3**, 987 (2012), arXiv: 1205.3106 [cond-mat.mes-hall].

[6] A.B. Shkarin et al, *Optically Mediated Hybridization between Two Mechanical Modes*, Phys. Rev. Lett. **112**, 013602 (2014), arXiv:1306.0613 [physics.optics].

[7] K. Audenaert, J. Eisert, M.B. Plenio & R.F. Werner, *Entanglement properties of the harmonic chain*, Phys. Rev. A **66**, 042327 (2002), arXiv:quant-ph/0205025.

[8] M.B. Plenio, J. Hartley & J. Eisert, *Dynamics and manipulation of entanglement in coupled harmonic systems with many degrees of freedom*, New J. Phys. **6**, 36 (2004), arXiv:quant-ph/0402004.

[9] M. Plenio & F.L. Semião, *High efficiency transfer of quantum information and multiparticle entanglement generation in translation-invariant quantum chains*, New J. Phys. **7**, 73 (2005), arXiv:quant-ph/0407034.

[10] A. Asadian, D. Manzano, M. Tiersch, and H.J. Briegel, *Heat transport through lattices of quantum harmonic oscillators in arbitrary dimensions*, Phys. Rev. E **87**, 012109 (2013), arXiv:1204.0904[quant-ph].

[11] E.A. Martinez, and J.P. Paz, *Dynamics and Thermodynamics of Linear Quantum Open Systems*, Phys. Rev. Lett. **110**, 130406 (2013), arXiv:1207.4256[quant-ph].

[12] N. Freitas and J.P. Paz, *Analytic solution for heat flow through a general harmonic network*, Phys. Rev. E. **90**, 042128 (2014), arXiv:1409.2904[quant-ph].

[13] F. Nicacio, A. Ferraro, A. Imparato, M. Paternostro & F.L. Semião, *Thermal transport in out-of-equilibrium quantum harmonic chains*, Phys. Rev. E **91**, 042116 (2015), arXiv:1410.7604[quant-ph].

[14] J.F. Leandro & F.L. Semião, *Creation and localization of entanglement in a simple configuration of coupled harmonic oscillators*, Phys. Rev. A **79**, 052334 (2009), arXiv:0905.0430[quant-ph].

[15] A. Carlisle, L. Mazzola, M. Campisi, J. Goold, F. L. Semião, A. Ferraro, F. Plastina, V. Vedral, G. De Chiara & M. Paternostro, *Out of equilibrium thermodynamics of quantum harmonic chains*, arXiv:1403.0629[quant-ph].

[16] F. Nicacio, R.N.P. Maia, F. Toscano & R.O. Vallejos, *Phase space structure of generalized Gaussian cat states*, Phys. Lett. A **374**, 4385 (2010), arXiv:quant-ph/1002.2248[quant-ph].

[17] F. Nicacio, K. Furuya & F. L. Semião, *Motional entanglement with trapped ions and a nanomechanical resonator*, Phys. Rev. A **88**, 022330 (2013), arXiv:1212.0711[quant-ph].

[18] A.M. Ozorio de Almeida, *The Weyl representation in classical and quantum mechanics*, Phys. Rep. **295**, 265 (1998).

[19] R.G. Littlejohn, *The Semiclassical Evolution of Wave Packets*, Phys. Rep. **138**, 193 (1986).

[20] M. de Gosson, *Symplectic Geometry and Quantum Mechanics* (Birkhäuser, Basel, series "Operator Theory: Advances and Applications", 2006).

[21] J. Williamson, *On the Algebraic Problem Concerning the Normal Forms of Linear Dynamical Systems*, Amer. J. Math. **58**, 141 (1936).

[22] J.J. Sakuray, *Modern Quantum Mechanics* (Addison-Wesley, Reading, 1994); C.C.-Tannoudji, B. Diu & F. Laloë, *Quantum Mechanics* (Wiley-VCH, Singapore, 2005);

[23] D. Kulkarni, D. Schmidt & S.-K. Tsui, Linear Algebra and its Applications **297**, 63 (1999).

[24] H. Scutaru, *Fidelity for displaced squeezed thermal states and the oscillator semigroup*, J. Phys. A: Math. Gen. **31**, 3659 (1998), arXiv:quant-ph/9708013.

[25] R. Simon, N. Mukunda & B. Dutta, *Quantum-noise matrix for multimode systems: $U(n)$ invariance, squeezing, and normal forms*, Phys. Rev. A **49**, 1567 (1994).

[26] F. Galve, A. Mandarino, M.G.A. Paris, C. Benedetti & R. Zambrini, *Microscopic description for the emergence of collective dissipation in extended quantum systems*, arXiv:1606.03390 [quant-ph].